Earth-Science Reviews 221 (2021) 103790

Contents lists available at ScienceDirect

Earth-Science Reviews

journal homepage: www.elsevier.com/locate/earscirev

Late Cretaceous to Early Cenozoic extension in the Lower Yangtze region (East China) driven by Izanagi-Pacific plate subduction

Xi Xu [a,b,c,d,*], Andrew V. Zuza [e], Lin Chen [f], Weilin Zhu [c,g], An Yin [d], Xiaowei Fu [c], Shunli Gao [h], Xuhui Xu [i], Xingtao Kuang [a], Fengqi Zhang [b], Lei Wu [b], Xiubin Lin [b], Hanlin Chen [b], Shufeng Yang [b]

[a] China Aero Geophysical Survey and Remote Sensing Center for Natural Resources, China Geological Survey, Beijing 100083, China
[b] School of Earth Sciences, Zhejiang University, Hangzhou 310027, China
[c] School of Ocean and Earth Sciences, Tongji University, Shanghai 200092, China
[d] Department of Earth, Planetary, and Space Sciences, University of California-Los Angeles, Los Angeles, CA 90925, USA
[e] Nevada Bureau of Mines and Geology, University of Nevada, Reno, NV 89557, USA
[f] State Key Laboratory of Lithospheric Evolution, Institute of Geology and Geophysics, Chinese Academy of Sciences, Beijing, 100029, China
[g] China National Offshore Oil Corporation (CNOOC), Beijing 100010, China
[h] China National Offshore Oil Corporation (CNOOC)-China Limited (Shanghai), Shanghai 200092, China
[i] SINOPEC Petroleum Exploration and Production Research Institute, Beijing 100083, China

ARTICLE INFO

Keywords:
East Asia
Lower Yangtze region
Extensional tectonics
Izanagi-Pacific plate
Oceanic slab subduction
Big mantle wedge

ABSTRACT

The intracontinental response to plate-boundary and mantle processes, such as subduction or continental collisions, is an important topic in the Earth Sciences. Cretaceous to Cenozoic extension across East China is related to the interaction between the Asian continental lithosphere and western Pacific oceanic subduction system, and the associated intra-plate structures and basins provide robust temporal and spatial records of regional continental deformation. Although extension may primarily be driven by slab rollback and/or back-arc opening, mid-ocean-ridge subduction may have played a significant role in this process. To explore how the western Pacific subduction system impacts intracontinental deformation across East China, we use onshore-offshore geological records, geophysical survey observations, and time-dependent Pacific plate models to document the temporal and spatial variation of continental deformation in the Lower Yangtze region adjacent to the Yellow Sea. Based on our compilation, we argue that mantle-wedge convection, with coupled subduction of the trench-parallel Izanagi (Paleo-Pacific)-Pacific mid-ocean ridge, exerts a first-order control on extensional deformation in East China. Beneath eastern China, the mantle wedge history consists of two phases: (1) initial development of the mantle wedge as the Cretaceous Izanagi slab transitioned from flat-slab to steep subduction; and (2) mature mantle wedge convection during Cenozoic subduction of the Pacific plate. Relatively steep subduction of the progressively younging Izanagi plate during the Late Cretaceous-Paleocene resulted in strong mantle convection and coupled upper plate extension in eastern China. The collision of the Izanagi-Pacific plate ridge system with the trench resulted in a magmatic gap and short-lived uplift of eastern China. Following this, subduction of the rapidly aging Pacific plate resulted in a larger, but relatively weaker, mantle convection cell that drove weaker upper plate extension. The vigor of wedge mantle convection was modulated by the age of the Pacific subducting slab, which directly influenced the formation and evolution of intracontinental extension and sedimentary basins across eastern China. The pre-existing Triassic Tan-Lu fault zone has reactivated since the Late Eocene (ca. 40 Ma) due to westward subduction of the Pacific slab to partition strain between extensional dextral faulting in the Bohai Bay and Lower Yangtze basins, thereby diversifying Cenozoic lithospheric extensional deformation in eastern China. Several major Cenozoic extensional basins spatially correlate with the Triassic Sulu orogenic belt, which we interpret to suggest that these basins are underlain by the older and fragmented orogenic basement that acted as mechanically weak zones for localized high-magnitude extension. We present a comprehensive

* Corresponding author at: China Aero Geophysical Survey and Remote Sensing Center for Natural Resources, China Geological Survey, Beijing 100083, China.
E-mail addresses: winbreak@163.com, lexus.phd@gmail.com (X. Xu).

https://doi.org/10.1016/j.earscirev.2021.103790
Received 27 March 2021; Received in revised form 26 August 2021; Accepted 31 August 2021
Available online 2 September 2021

tectonic model that relates intracontinental deformation to subduction zone dynamics, particularly emphasizing the importance of the age of the subducting slab, thus providing a coherent geologic process to explain the deformation kinematics in eastern China and the diversity of observed Mesozoic-Cenozoic basin formation.

1. Introduction

The coupling between oceanic plates and the overriding continental lithosphere at continental margins along convergent plate boundaries generates intraplate deformation on the Earth's surface (e.g., DeCelles, 2004; Liu and Nummedal, 2004; Lallemand et al., 2005; Clark et al., 2008; Liu et al., 2008; Cawood et al., 2009; Dilek and Altunkaynak, 2009; Yin, 2010; Liu et al., 2011; Yang, 2013; Zhang et al., 2017; Liu et al., 2017a; Müller et al., 2016; Liu et al., 2021a, 2021b, 2021c, 2021d; Li et al., 2019; Suo et al., 2020). Modern studies in continental tectonics seek to understand how intracontinental deformation responds to edge-driven plate-boundary conditions versus the release of excess intra-plate gravitational potential energy (e.g., Sonder and Jones, 1999; Yin, 2010; Yang, 2013; Liu et al., 2017a). Intra-plate structures and volcanic and sedimentary records within the continents provide robust archives of the evolving history of plate boundaries, including variations in the mode, direction, and velocity of plate subduction (Dickinson et al., 1978; Wilson, 1991; Li and Li, 2007; Liu et al., 2013; Ingersoll, 2019; Wu and Wu, 2019; Yang et al., 2020; Liu et al., 2017a; Liu et al., 2021c, 2021d). In particular, it remains unclear how well geologic observations at the Earth's surface record changes and reorganization of plate kinematics and inter-plate dynamics.

The tectonics of East Asia involve the westward subduction of the (Paleo-) Pacific Ocean plate during the Mesozoic and Cenozoic, which led to magmatism and intra-plate deformation across eastern China (e.g., Ren et al., 2002; Yin, 2010; Liu et al., 2017a; Wu et al., 2019; Liu et al., 2021a). Widely accepted models for East China relate both sweeps in Mesozoic-Cenozoic plutonism and intracontinental extension in the Late Cretaceous-Cenozoic to progressive eastward rollback of the subducting oceanic lithosphere (e.g., Watson et al., 1987; Ren et al., 2002; Xu, 2007; Yin, 2010; Zhu et al., 2021). A prominent north-trending lineament divides East Asia, referred to as the North-South Gravity Lineament (NSGL), with abrupt variations in topography, crustal thickness, gravity, and Mesozoic-Cenozoic basin sedimentation on either side (e.g., Xu, 2007; Liu et al., 2021a) (Fig. 1). This major tectonic transition zone probably formed in the Late Mesozoic because Cenozoic extensional basins are primarily restricted to the east of the NSGL, whereas Mesozoic syn-extension sediments are observed across lineament (e.g., Ren et al., 2002; Liu et al., 2017a; Liu et al., 2021a). Indeed, both magmatism and lithospheric thinning stretch from the Pacific trench to the NSGL, and Liu et al. (2021a) demonstrated how the NSGL formed during Paleo-Pacific subduction dynamics. The patterns of

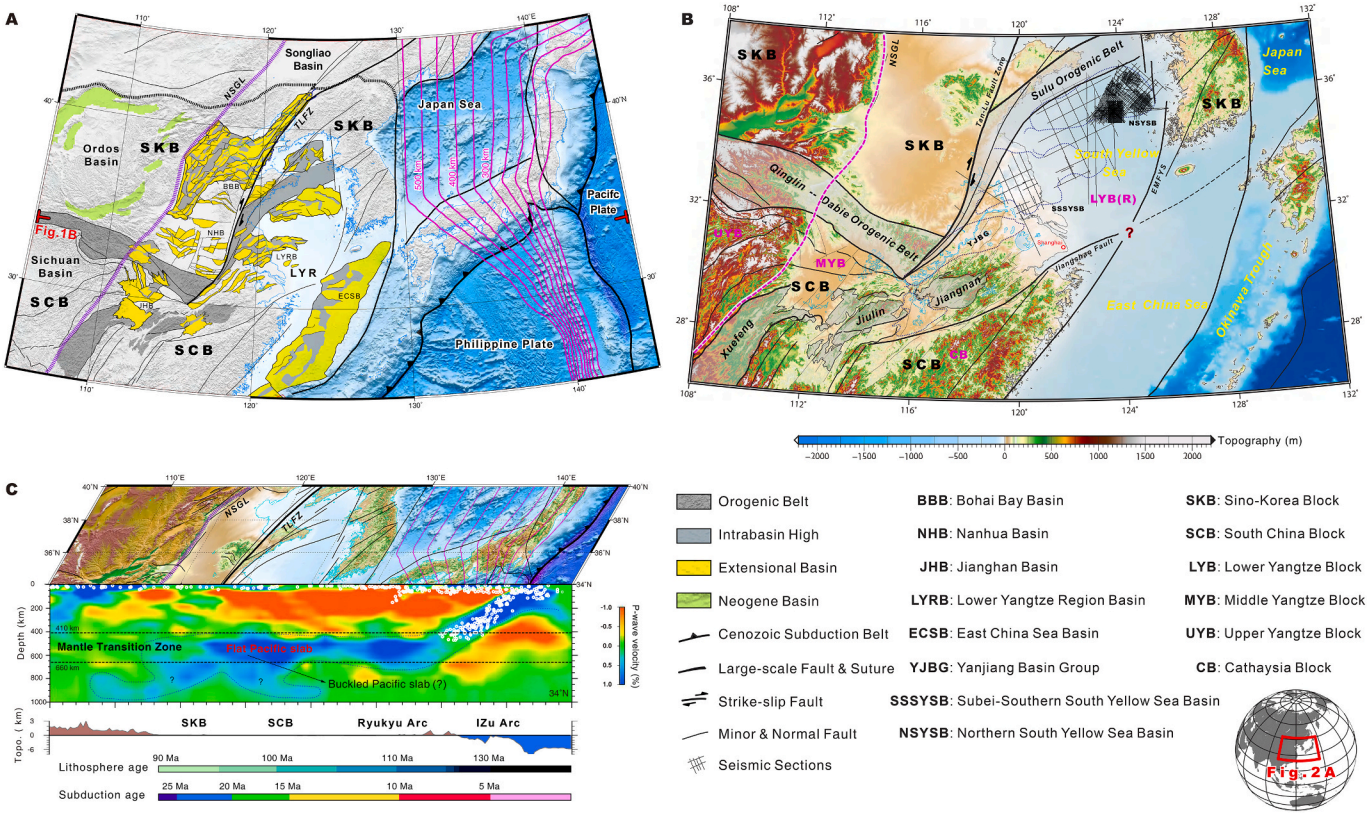

Fig. 1. (A) Late Mesozoic and Early Cenozoic extensional basins of East China and the overall tectonic framework. Pink dotted line indicates the Daxing'anling-Taihangshan-Wulingshan North-South Gravity Lineament (NSGL) (Xu, 2007). The thick pink lines denote depth contours of the present upper boundary of the subducting Pacific slab (Liu et al., 2017b). LYR, Lower Yangtze region. (B) Tectonic setting of the Lower Yangtze Block and its surrounding environments overlain on a topographic map. Blue dotted lines indicate the distribution of extensional sedimentary basins, including the Yangjiang basins group (YJBG), Subei-Southern South Yellow Sea basin (SSSYSB) and Northern South Yellow Sea basin (NSYSB), comprised the Lower Yangtze region basin (LYRB). EMFYS, East marginal fault of South Yellow Sea. (C) Vertical cross-section of P-wave tomography across the eastern China-western Pacific at the latitude 34°N (after Liu et al., 2017b). The red and blue colors correspond to low and high velocity perturbations, respectively. The subducting Pacific lithosphere ages and the subducting ages of the Pacific slab from the East China (the west) to the trench axis (the east) are all shown by color bars, with a scale (in Ma) in the upper left.

widespread Middle Jurassic to Early Cretaceous magmatism suggest westward flattening of the Jurassic slab, inland to the NSGL, followed by Cretaceous eastward rollback that extended the East Asia lithosphere (e.g., Liu et al., 2013; Liu et al., 2017a; Wu et al., 2019; Liu et al., 2019; Liu et al., 2021a, 2021b).

This envisioned tectonic evolution broadly explains the known geologic history of East Asia, but in detail, structural and stratigraphic observations within the distributed extensional basins nested in East China (Fig. 2), such as the Bohai Bay and Lower Yangtze Basins (Fig. 1A and 1B), are difficult to reconcile with this monotonic back-arc extension model. Complicating this simple conceptual model is the variable history of the major north-striking lithosphere-scale Tan-Lu Fault Zone (TLFZ), which dissects East China, with variable kinematics throughout the Cenozoic (e.g., Grimmer et al., 2002; Hsiao et al., 2004; Mercier et al., 2013a, 2013b; Huang et al., 2015, 2018), and early Cenozoic subduction of the mid-ocean ridge that divided the Izanagi (Paleo-Pacific) and Pacific oceanic plates (Whittaker et al., 2007; Müller et al., 2016; Ma et al., 2019; Liu et al., 2021d). Therefore, Late Mesozoic-Early Cenozoic intraplate deformation in eastern China may be more complex than previously considered, involving strongly coupled intracontinental strike-slip and extensional deformation driven by the complex western Pacific subduction history.

In addition, a >1,000-km long seismically-observed stagnant slab in the mantle transition zone (MTZ) beneath Northeast Asia (Fig. 1C) (e.g., Huang and Zhao, 2006; Wei et al., 2012; Chen et al., 2017) is thought to be a robust observation of the subducted Pacific plate. The present geometry resulted from the history of westward subduction of the Izanagi oceanic plate in the Mesozoic, the Izanagi-Pacific mid-ocean ridge, and subsequently the Pacific plate in the Cenozoic (Whittaker et al., 2007; Seton et al., 2015; Wu and Wu, 2019; Liu et al., 2021d). The overriding intracontinental extension and associated sedimentary basins formed in response to the evolving subduction history of the Izanagi-Pacific oceanic slabs beneath East China. However, there is no unified geodynamic/tectonic model linking the various regional events together. The following important questions based on the existing geologic record remain unanswered: (1) Why is the spatial-temporal record of

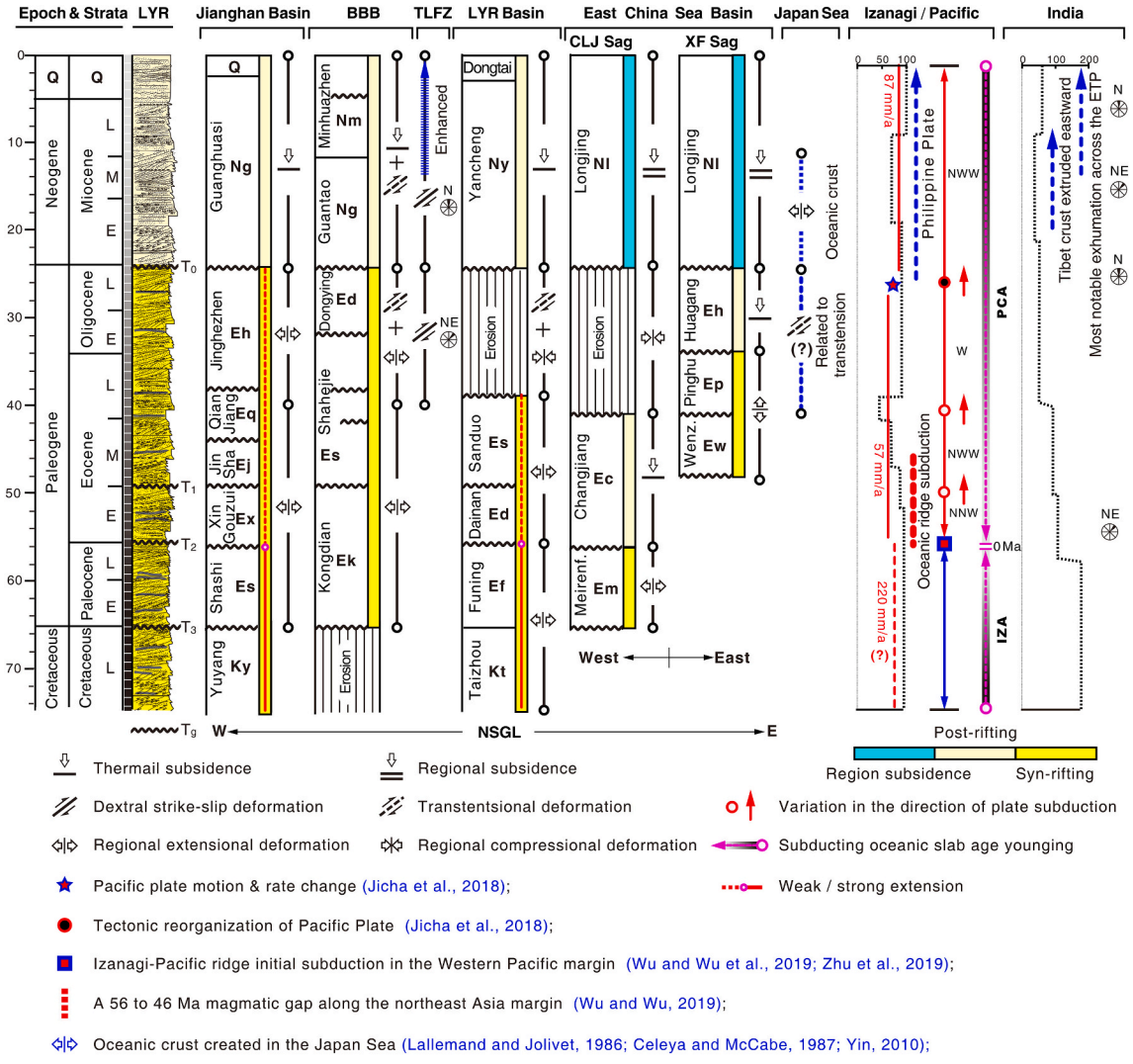

Fig. 2. Correlation chart of late Mesozoic and Cenozoic tectonic-sedimentary evolution of the extensional basins in East China and related plate geodynamic boundaries. Data sources for the evolution of these basins: Jianghan (e.g., Wu et al., 2018a, 2018b), Bohai Bay (e.g., Qi and Yang, 2010; Zhu et al., 2010; Huang et al., 2012, 2018) and East China Sea (Zhu et al., 2019) basins, as well as the Tan-Lu fault zone (TLFZ) (e.g., Huang et al., 2015) and the Japan Sea (e.g., Lallemand and Jolivet, 1986; Celaya and McCabe, 1987; Jolivet et al., 1994; Yin, 2010). T_0, T_1, T_2, T_3 and T_g are the sedimentary unconformities within the Lower Yangtze region basin. The convergence rates between the Pacific and Indian and Eurasian plates are from Northrup et al. (1995) and Lee and Lawver (1995), respectively. Related tectonic events and evolution are derived from the literature: Izanagi (IZA) and Pacific (PAC) Plates (e.g., Wu et al., 2016; Müller et al., 2016; Jicha et al., 2018; Wu and Wu, 2019; Zhu et al., 2019), Philippine Sea plate (e.g., Wu et al., 2016; Ma et al., 2019; Liu et al., 2021d) , Tibet (e.g., Zhu and Yin, 2016; Webb et al., 2017; Bian et al., 2020), and the Eastern Tibetan Plateau (ETP) (e.g., Ouimet et al., 2010; Tian et al., 2015; Fu et al., 2021).

sedimentation in East China is so diverse (e.g., Ren et al., 2002; Meng et al., 2019; Liu et al., 2017a; Zhu et al., 2019), which implies complex multifaceted plate-boundary forcing rather than a simple scenario of monotonic slab rollback? (2) Why did the TLFZ switch kinematics during the Cenozoic (e.g., Jiang et al., 2019; Mercier et al., 2007), apparently out of sync with basin sedimentation in the Bohai Bay basin to its west and the Lower Yangtze basin to its east? (3) Why did all of the sedimentary basins in eastern China transform from syn-rift sedimentation to post-rift, thermal subsidence-related sedimentation at ca. 25 Ma (e.g., Ren et al., 2002; Yin, 2010; Liu et al., 2017a) despite continuous westward subduction of the Pacific plate and contemporaneous spreading of the Japan Sea (e.g., Jolivet et al., 1994; Yang et al., 2018a, 2018b)? To address these long-held questions, a comprehensive synthesis of basin sedimentation, structural evolution, and geophysically derived subsurface information is required. However, previous studies are mainly focused on either individual sedimentary basins or discrete fault structures, such as the TLFZ, (e.g., Qi and Yang, 2010; Shinn et al., 2010; Huang et al., 2015; Xu et al., 2015a, 2015b; Wu et al., 2018a; Zhu et al., 2018). Comprehensive reviews address some of these questions as part of broader studies of East Asia or China (e.g., Ren et al., 2002; Yin, 2010; Liu et al., 2017a; Liu et al., 2021a; Liu et al., 2021d), but these so far neglect the Lower Yangtze basin due to the scarcity of reliable geological-geophysical data.

In this study, we synthesize multidisciplinary observations, including onshore-offshore geological and geophysical data, as well as time-dependent tectonic boundary conditions provided by well-constrained western Pacific plate models (e.g., Müller et al., 2016; Wu and Wu, 2019; Jicha et al., 2018; Ma et al., 2019; Liu et al., 2021d), to decipher the temporal and spatial variations of crustal rifting in the Lower Yangtze region, eastern China. First, we synthesize the scale and timing of lateral and vertical variations in basin geometry, stratigraphic record, and structural architecture by using 2D seismic and borehole data. Second, we develop a comprehensive correlation scheme across the ~1000-km-wide area that includes the Bohai Bay, Jianghan and East China Sea basins to integrate the knowledge of major basin sedimentation history and the kinematics of key basin-bounding fault structure. From this synthesis, we propose a new model for the extensional history in eastern China that is based on coupled lithosphere-mantle dynamics and west-dipping Pacific subduction system.

2. Data and methods

Our tectonic synthesis presented in this study is an integrated compilation of multidisciplinary observations, incorporating a range of geological and geophysical datasets, organized for each of the important sedimentary basins such as the Bohai Bay, Jianghan, Lower Yangtzem and East China Sea basins, tectonic units, and major fault zones in eastern China. These data are then compared with the inferred history of the Izanagi-Pacific plate (Fig. 1). The geographic locations, names, and the unit geometries discussed in this work are provided in Fig. 1. Sedimentary records, major structures, and fault activity of the major basins are summarized in Fig. 2 based on previous syntheses (e.g., Qi and Yang, 2010; Zhu et al., 2010; Xu et al., 2015a, 2015b; Wu et al., 2018a; Zhu et al. 2019). The marginal-sea opening history and kinematic development (e.g., Lallemand and Jolivet, 1986; Celaya and McCabe, 1987; Jolivet et al., 1989, 1990, 1994; Liu et al., 2001) and plate motion information (e.g., Müller et al., 2016; Wu and Wu, 2019; Jicha et al., 2018) are temporally correlated with the records summarized in Fig. 2.

Compiled data include 2-D seismic reflection profiles, satellite-based gravity-aeromagnetic data, borehole data, and field observations. We present new high-resolution seismic data with grid spacing of 1 km × 1 km and 2 km × 2 km to interpret the basin structure across the northern part of the Yellow Sea. The seismic sections and borehole data, both onshore and offshore, are approved for release for research purposes by the China Petrochemical Corporation (Sinopec) and China National Offshore Oil Corporation (CNOOC). Structural boundaries and geologic contexts of the major basins are digitized from the recently available data (e.g., Qi and Yang, 2010; Zhu et al., 2012; Liu et al., 2017a, 2017b, Zhu et al., 2019; Wu, 2018a,b). A few minor basins, such as Nanhua (Zhu et al., 2012) and Nanxiang (Shen et al., 2018) basins, are also included in the synthesis.

The kinematic and subduction history of the Izanagi-Pacific plate used in this study were determined from recent datasets of Mesozoic-Cenozoic intrusions along the east Asian margin, updated ages for the Hawaiian-Emperor chain in the Pacific Ocean and plate rate estimates, and tectonic plate reconstructions and associated kinematic models (e.g., Hall, 2002; Whittaker et al., 2007; Müller et al., 2016; Torsvik et al., 2017; Wu and Wu, 2019; Jicha et al., 2019; Ma et al., 2019; Liu et al., 2021d). We have also systematically compiled other tectonic datasets, including Mesozoic magmatism in eastern China (e.g., Charles et al., 2013; Lin et al., 2013; Wu et al., 2019; Liu et al., 2019), the structural history of the Tan-Lu fault zone (e.g., Zhao et al., 2016; Huang et al., 2015, 2018), and reconstructions of the opening of the Japan Sea (e.g., Lallemand and Jolivet, 1986; Celeya and McCabe, 1987; Jolivet et al., 1994; Yin, 2010).

3. Mesozoic-Cenozoic tectonics in the Lower Yangtze region

The geology of eastern China is expressed by a complex mosaic of tectonically accreted continental fragments, inherited from the evolution of cyclical Gondwana-derived terranes and the prolonged convergence between the Paleo-Pacific and Eurasian plates (Metcalfe, 2006; Seton et al., 2012; Zahirovic et al., 2014; Liu et al., 2017a; Liu et al., 2021a, 2021d) that are currently separated by suture and strike-slip fault zones. The Lower Yangtze region of eastern China is uniquely positioned in a tectonic framework that has been strongly affected by Mesozoic continental collisions and Mesozoic-Cenozoic west-dipping oceanic subduction (Fig. 1; Fig. 2). The overall lithospheric structure of east China resulted from the collision of various continents, such as the South China and Sino-Korean blocks. Numerous collision models have been proposed by previous studies (e.g., Yin and Nie, 1993; Xu and Zhu, 1994; Zhang, 1997; Chang and Park, 2001; Wan, 2013; Wu, 2005; Suo et al., 2014; Li et al., 2012; Xu et al., 2015a), corresponding to a series of collisional and suturing events (Fig. 3). The amalgamation of both blocks exerted a crucial role in shaping the tectonic framework of the eastern Chinese continent (Fig. 4). Geographically, the Lower Yangtze region encompasses the Yangtze River area and Jiangsu Plain, and extends to the South Yellow Sea. A high-resolution digital elevation map clearly depicts surface lineaments of large-scale intracontinental faults in the Lower Yangtze region, such as the Tan-Lu and Jiangshao faults, as shown in Fig. 1B. In particular, the TLFZ extends as far as the Shandong Peninsula to the north and separates the Dabie and Sulu orogenic belts created by the collision between the Sino-Korea and South China blocks during the Triassic; the TLFZ has been commonly considered as a prominent dextral strike-slip fault since the Cenozoic (e.g., Xu et al., 1987; Grimmer et al., 2002; Mercier et al., 2007; Xu and Zhu, 1994). The Lower Yangtze region is separated from the Korean Peninsula by the east marginal fault of South Yellow Sea (Fig. 1B), which was observed based on well-constrained geological and geophysical observations from the early 2000s (e.g., Chang and Zhao, 2012; Hao et al., 2003, 2007; Xu et al., 2008a).

3.1. Mesozoic tectonics and deformation within and around the Lower Yangtze region

The collision between the Sino-Korea and South China blocks occurred in the Late Triassic and Early Jurassic (also known as the Indosinian Period or Movement in Chinese literature), and a wide range of tectonics models have been published on this orogen (e.g., Xu and Zhu, 1994; Yin and Nie, 1993; Zhang, 1997; Chang and Park, 2001; Zhang et al., 2004; Liu et al., 2005, 2015; Wan, 2013; Wu, 2005; Suo et al., 2014; Li et al., 2012a, 2012b; Xu and Gao, 2015a) (Fig. 3).

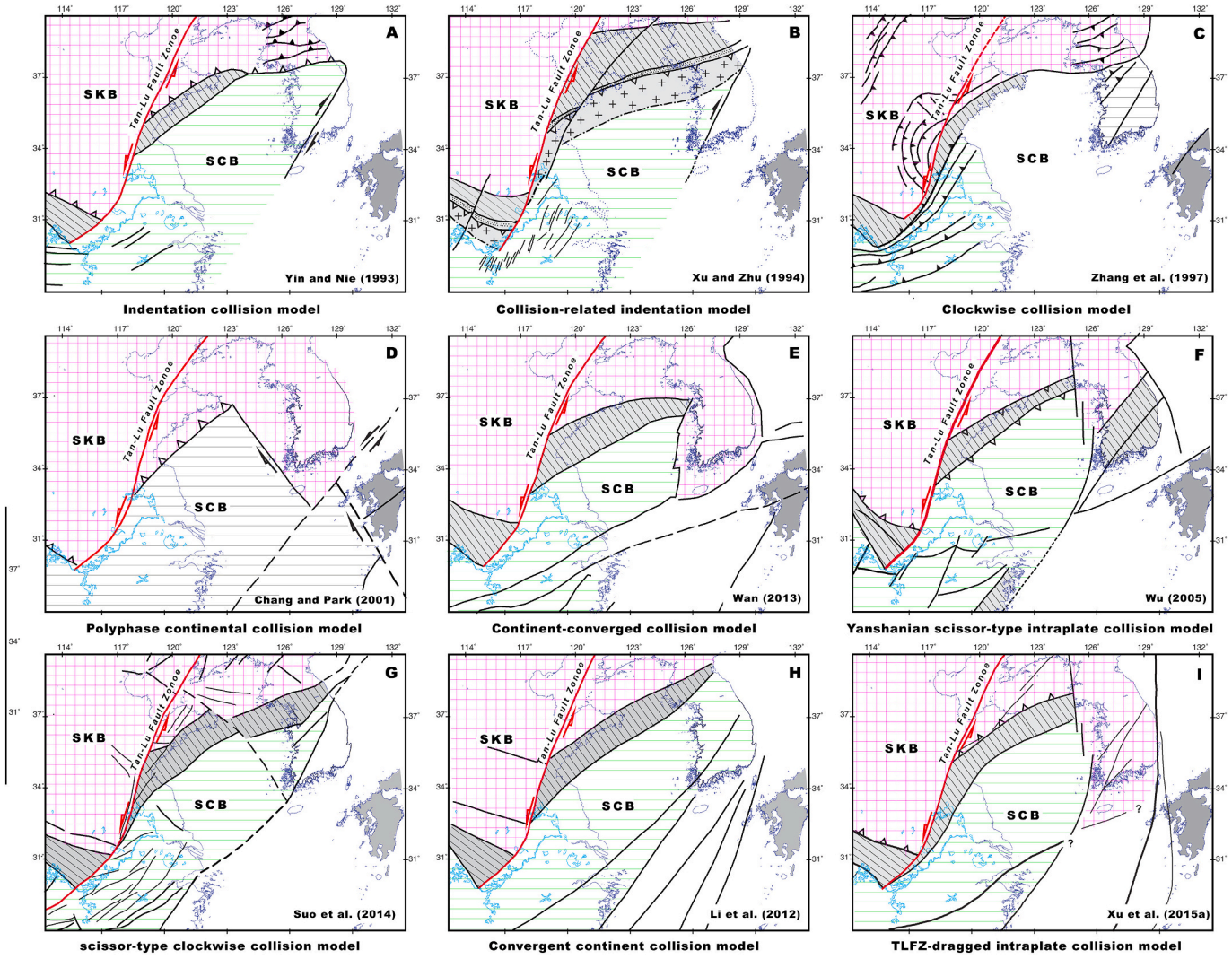

Fig. 3. Tectonic models for the correlation between the Sino-Korean Block (SKB) and South China Block (SCB). Models from A to I are: Indentation collision model (Yin and Nie, 1993), Collision-related Indentation model (Xu and Zhu, 1994), Clockwise collision model (Zhang, 1997), Polyphase continental collision model (Chang and Park, 2001), Continent-converged collision model (Wan, 2013), Yanshanian scissor-type Intraplate collision model (Wu, 2005), Scissor-type clockwise collision model (Suo et al., 2014), Convergent continent collision model (Li et al., 2012a, 2012b) and TLFZ-dragged intraplate collision model (Xu and Gao, 2015a), respectively. TLFZ–Tan-Lu Fault Zone.

Prominent models include a scissor-type model where the South China block diachronously sutured to the Sino-Korean block from east to west, accompanied by ~70° clockwise rotation (Li et al., 2007; Zhao and Coe, 1987; Liu et al., 2017a, 2017b; Chang and Zhao, 2012) and an indentation model where the northeast South China block indented into the eastern Sino-Korean block (e.g., Yin and Nie, 1993). The collision of these two blocks generated strike-slip faults and the composite Dabie-Sulu orogenic belt (Fig. 4A). Progressive orogeny generated high/ultrahigh-pressure metamorphic rocks that were subsequently exhumed between ~220 and 200 Ma (e.g., Xu, 2003; Faure et al., 2003; Hacker et al., 2006a,b; Zheng et al., 2003, 2005; Yang et al., 2005). Furthermore, ca. 192-188 Ma muscovite $^{40}Ar/^{39}Ar$ ages from the TLFZ (Zhu et al., 2004, 2005) reveal that the fault accommodated motion between the Sino-Korean and South China blocks during the Late Jurassic, probably the result of continuous flat subduction of the Paleo-Pacific (Izanagi) oceanic plate (e.g., Wu et al., 2019) or the newly interpreted Yanshanian composite-slab flat subduction (e.g., Liu et al., 2021b) beneath East China. Coeval with the Sulu orogenic belt was the development of the Jiangnan and Jiuling orogenic belts that were reactivated from an early Paleozoic suture between the Cathaysian and the Yangtze blocks that bounded the current southern edge of the Lower Yangtze Block (Charvet et al., 1996; Shu and Charvet, 1996; Shu et al., 1991) (Figs. 5 and 6), which generated local north-trending folding and thrusting in the south of the Lower Yangtze region (Fig. 4B).

As a result, the Sulu orogenic belt was tectonically transported northward ~500 km relative to the Dabie orogenic belt along the northeast-striking TLFZ, with displacement accumulating until the Early Cretaceous (e.g., Xu et al., 1987; Xu and Zhu, 1994; Zhu et al., 2005; Wang, 2006) (Figs. 1B and 4B). Integrated geological and geophysical observations, including a large dataset of high-resolution petrological, gravimetric, and magnetic data (Fig. 5), show the current extent of the Dabie and Sulu orogenic belts displaced by the imaged TLFZ. The Sulu orogenic belt was displaced from the Dabie orogenic belt by sinistral strike-slip movement on the TLFZ, displaying a dragged arc-like geometry varying from NNE-striking to NEE-striking from the west to the east (Fig. 5). Crustal shortening related to this collision and strike-slip displacement can be examined via a series of published geologic cross sections (Wang, 2012; Zhang, 2014), which reveal decreasing shortening from west to the east across the Yanjiang region (Fig. 6). This strain gradient was driven by greater deformation close to the collisional belt and TLFZ, and continued Sino-Korea-South China block convergence (e.g., Dong et al., 2013) and collision-induced stress (Fig. 4 and

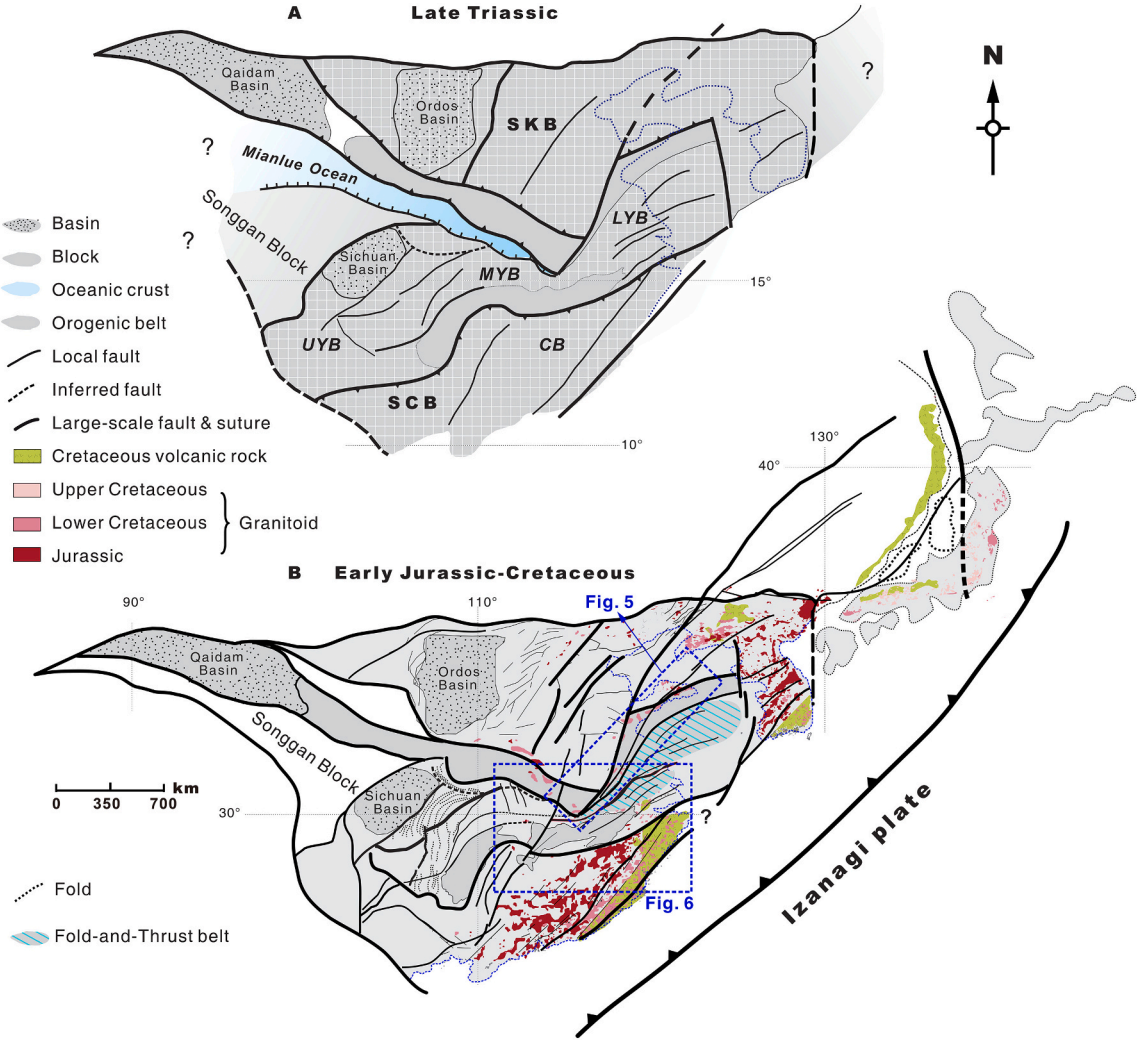

Fig. 4. (A) Sketch map showing the collisional and suturing features of the South China Block (SCB) and Sino-Korean Block (SKB) in the Late Triassic-Early Jurassic. Structures modified from Li et al. (2007), Li and Li (2007), Wan (2010), and Chang and Zhao (2012). The South China Block is commonly segregated into the Yangtze Block, including the Upper, Middle and Lower Yangtze Blocks (UYB, MYB and LYB, respectively), and the mobile block to the south, also known as the Cathaysia Block (CB). (B) Tectonic map showing the tectonic domains of the Lower Yangtze and its adjacent blocks in eastern China, especially Early Jurassic-Cretaceous reconstruction of the LYB and its environs. Magmatism compiled from Charles et al., 2013 and Lin et al., 2013. The position of the Japan Island was palinspastically restored (Lallemand and Jolivet, 1986; Jolivet et al., 1994; Liu et al., 2001; Hou and Hari, 2014).

Fig. 6). The Lower Yangtze block is bounded by a series of major fault zones and tectonically surrounded by the Sino-Korea, Upper-Middle Yangtze, and Cathaysia blocks. This configuration yields a wedge-shaped geometry, with a wide region in the east and narrow region in the west, which experienced internal extensional deformation during the Late Cretaceous and Cenozoic (Fig. 4B).

3.2. Basement framework

The pre-Cretaceous tectonics across the Lower Yangtze region consist of a fold-thrust belt that formed due to the Triassic-Jurassic Sino-Korea-South China block collision. South of the Sulu orogenic belt, the region was strongly deformed by north-directed contractional deformation (Fig. 4B), which developed fold-thrust belts that are presently observed beneath the Cenozoic sedimentary basin (Yao et al., 2010; Zhu et al., 1999), referred to as the Yangtze foreland fold-and-thrust belt (e.g., Li et al., 2012a, 2012b; Zhu et al., 1999). To the south of the Yangtze River, the north-verging folding and thrusting, related to the Jiangnan orogenic belt, resulted in deformation of the Neoproterozoic-Paleozoic sedimentary cover rocks (Shu et al., 2008; Wang, 2018). In the region along the Lower Yangtze River juxtaposed by the Mesozoic Sulu and Jiangnan orogenic belts, a double-foreland fold-thrust belt exists with oppositely verging thrusts (Figs. 4B and 6). Due to its proximity to the TLFZ, the strike of the structural lineaments close to the NNE-striking portion of the Sulu orogenic belt is curved to the south to trend NNE, whereas the structural traces away from the TLFZ vary from NNE to NEE from west to east, respectively (Fig. 7A).

Contractional structures formed by Triassic-Jurassic shortening are exposed across the inland surface and are concealed by the Cenozoic sedimentary cover beneath the Subei plain and South Yellow Sea (Fig. 7). Additionally, regional cross sections illustrate that the contractional and heterogeneous basement structures are overlain by fault-bounded sedimentary basins (Fig. 6) (Wang et al., 2012; Zheng et al., 2013). In turn, these basins are covered by undeformed Neogene and Quaternary strata. Large data sets are available for the Lower Yangtze region due to the development of oil/gas exploration at depth, but information about the Mesozoic pre-existing structural fabrics is still lacking, primarily because the resolution of the seismic reflection profiles prevents detailed interpretation and mapping of the blind thrusts within the basement (Figs. 9 and 10). Although it is difficult to determine the precise geometry and location of the pre-existing thrust faults, the onshore geology of the Lower Yangtze region provides the best

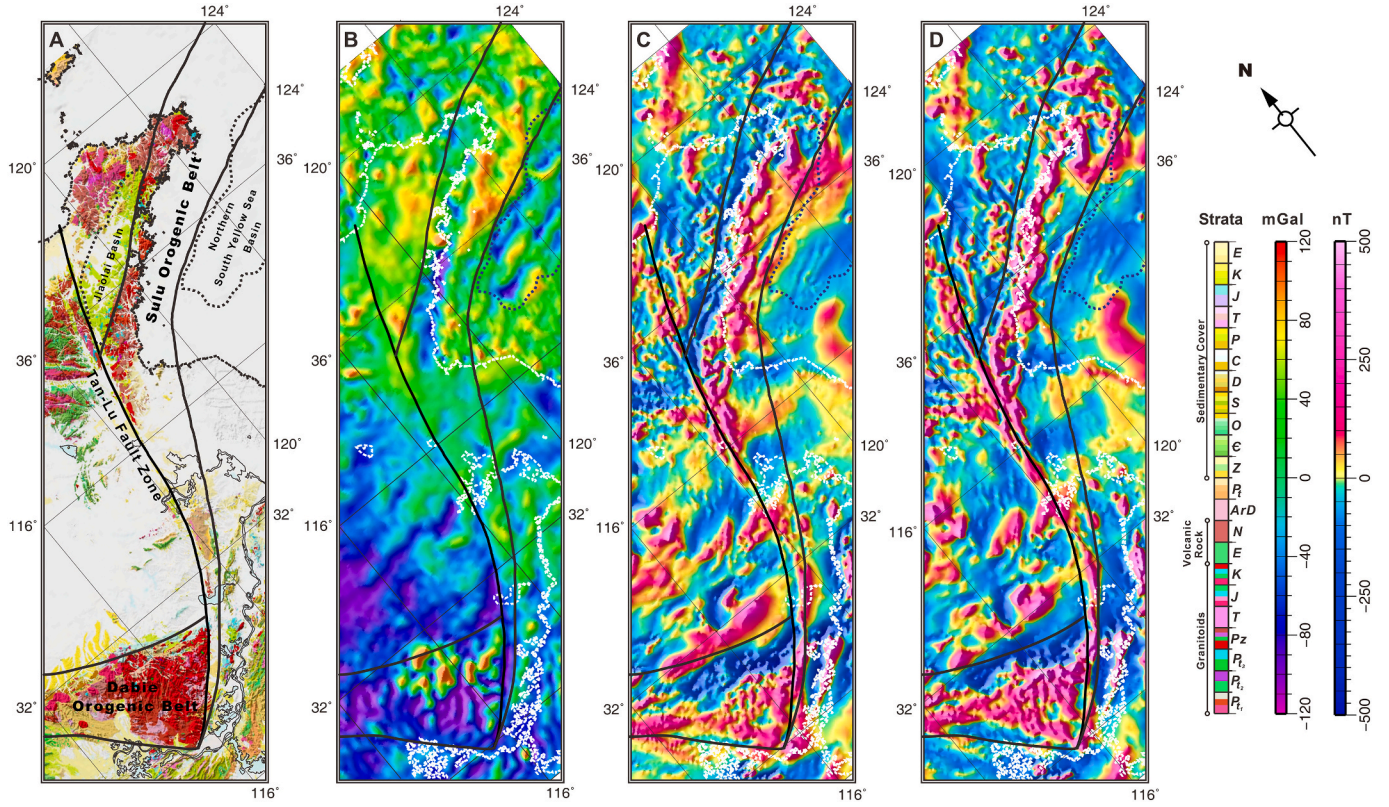

Fig. 5. Tectonic interpretations for the geometry of the Dabie-Sulu Orogen orogenic belt, based on various geological and geophysical datasets. (A) Geological and tectonic map of the Dabie-Sulu Orogen projected onto a digital elevation model. Geological map projected onto DEM is abbreviated as GDEM in this paper, mainly modified from the 1: 200,000 scale geological maps of Shandong, Jiangsu, Anhui, Zhejiang, Jiangxi and Hubei provinces (JXBGMR (Jiangxi Bureau of Geology and Mineral Resources), 1984; JSBGMR (Jiangsu Bureau of Geology and Mineral Resources), 1987; AHBGMR (Anhui Bureau of Geology and Mineral Resources), 1987; ZJBGMR (Zhejiang Bureau of Geology and Mineral Resources), 1989; HBBGMR (Hubei Bureau of Geology and Mineral Resources), 1990; SDBGMR (Shandong Bureau of Geology and Mineral Resources), 1991). Digital elevation from Becker et al. (2009). (B) Regional free-air gravity map (data from Sandwell et al., 2013). (C) Map of high-resolution aeromagnetic anomalies (data from Xiong et al., 2016) and (D) that after the reduction to the pole. Overlain on maps are topographic contours of 0 m (dotted black curves in Fig. 5A, and dotted white curves in the others), as well as the Yangtze River and lakes.

constraint of the nature of the heterogeneous basement. Evidence derived from offshore structural and geophysical data, such as the consistency in the thrust trend and strike of the normal fault (e.g., Ding et al., 2009; Zhu et al., 1999), trend of extensional structures (e.g., Shinn et al., 2010; Yao et al., 2010; Yoon et al., 2010), the regional trend of the Bouguer (and Free-air) gravity anomaly (e.g., Li et al., 2012a, 2012b; Zhang et al., 2007) and others, consistently demonstrates that the underlying structure and crustal anisotropy have a NNE-NEE orientation in the Subei plain and a NEE or nearly east-west orientation in the South Yellow Sea. This variation in orientation is consistent with the obtuse-angled change in trend of the Sulu orogenic belt (Fig. 7A). As mentioned above, the spatial-temporal correlation between the outcrop and subsurface geology demonstrate that the fault-bounded basins in the Lower Yangtze region developed atop a complex and heterogeneous basement. The basement includes multiple structural fabrics, most notably the Yangtze fold-thrust belt, which was a long-lived pre-existing weak zone, that was reactivated in the Cenozoic to control the occurrence, geometry, and fill of these basins (Fig. 7).

3.3. Sedimentary basins in the Lower Yangtze region

Present-day basins in the region have been active sedimentary basins since the Late Cretaceous. The Late Cretaceous-Paleogene basins, covered by Neogene-Quaternary sediments, are nested within the Lower Yangtze region, and distributed across an area of nearly 193,500 km^2 that experienced Late Mesozoic-Early Cenozoic crustal extension. We refer to this basin system as the Lower Yangtze region basin, which extends in a NE direction from onshore to offshore (Figs. 1A, 1B and 7B). Based on newly interpreted petroleum exploration data, this large basin system can be subdivided into three tectono-stratigraphic levels, exhibiting an evolution from early-stage coeval extension to late-stage thermal subsidence corresponding to the syn-rift and post-rift stages (Xu and Gao, 2015a; Xu et al., 2015a). Two regional unconformities separate the Upper Cretaceous-Paleogene strata from the overlying and underlying successions, respectively (Fig. 2). These three stratigraphic groups are commonly regarded as pre-, syn- and post-rift mega-sequences, separated by two mega-sequence unconformities (Fig. 2). The pre-Cretaceous sequences acted as the basement of the Lower Yangtze region basin is mainly composed of marine sedimentary and crystalline-metamorphic rocks (e.g., Ren et al., 2002; Xu and Gao, 2015a; Xu et al., 2015a, 2015b, 2018; Gao et al., 2015; Pang et al., 2018). These deposits are overlain by divergently configed strata, which were deposited during the Late Mesozoic-Early Cenozoic extension era. The Upper Cretaceous-Paleogene strata are developed in the basin, fed predominantly with alluvial and fluvial sediments with lacustrine deposits like siltstones and mudstones that are the major petroleum source rocks in all these basins (Shinn et al., 2010; Xu and Gao, 2015a; Xu et al., 2018). Extensional faulting involved differential tectonic subsidence, and abruptly diminished in the late Paleogene, followed by a clearly discernible regional thermal subsidence in the Neogene and Quaternary periods, which are termed the “depression” and “sag” phases in Chinese literature, respectively (e.g., Ren et al., 2002).

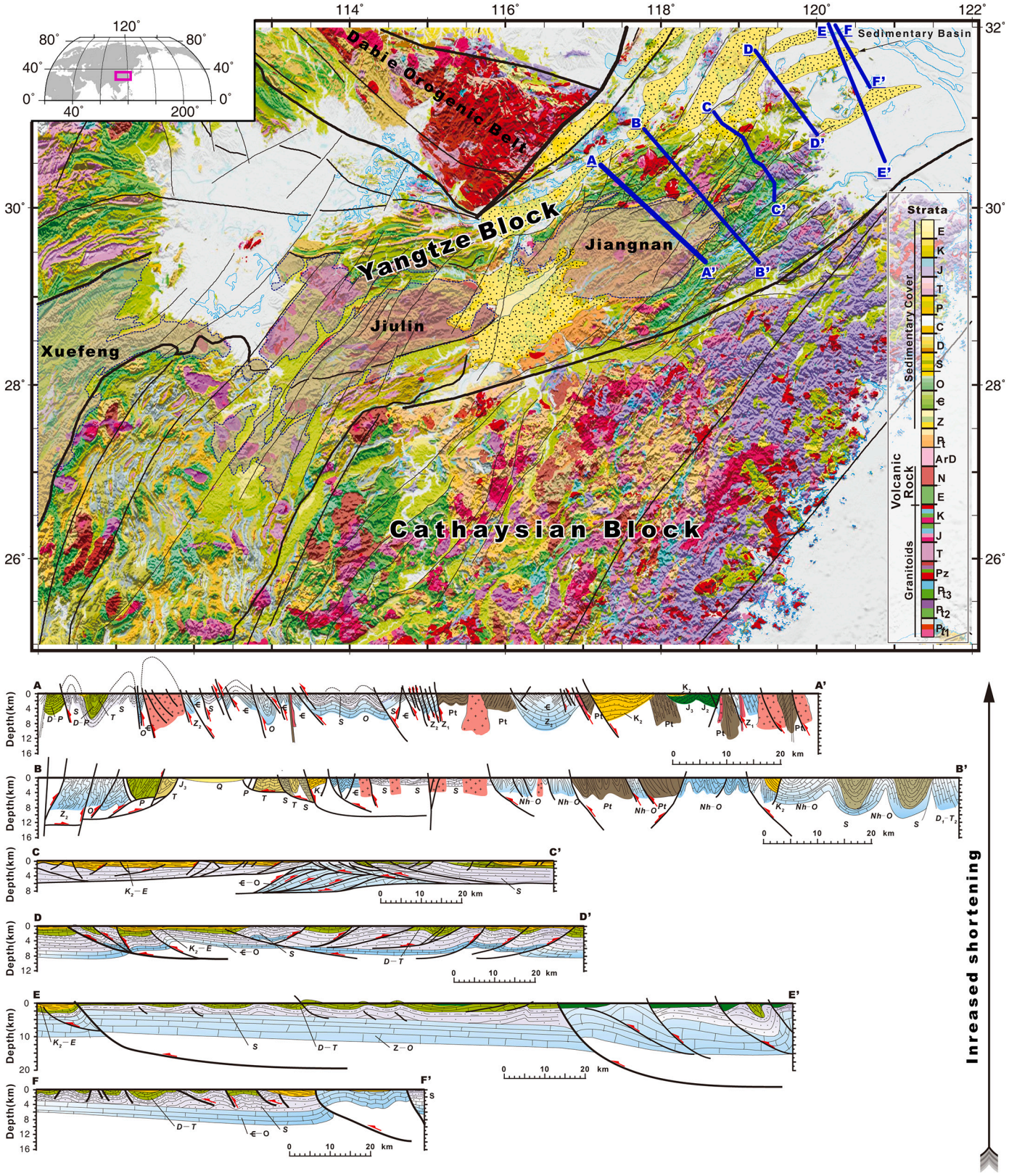

Fig. 6. Regional geological and structural maps of the western segment of the Lower Yangtze Block overlain on a digital elevation model (Becker et al., 2009). The black lines represent regional faults. The geometry and architecture of the onshore basins and faults are established by the topographic and stratigraphic indicators. The geological map is mainly modified from the 1: 200,000 scale geological maps of the Jiangsu, Anhui, Zhejiang, Jiangxi and Hubei provinces (JXBGMR (Jiangxi Bureau of Geology and Mineral Resources), 1984; AHBGMR (Anhui Bureau of Geology and Mineral Resources), 1987; ZJBGMR (Zhejiang Bureau of Geology and Mineral Resources), 1989; JSBGMR (Jiangsu Bureau of Geology and Mineral Resources), 1987; HBBGMR (Hubei Bureau of Geology and Mineral Resources), 1990). The five cross-sections from AA' to FF' are from Wang et al. (2012) and Zhang et al. (2013). Note the trend of increased shortening strain from east (F-F') to west (A-A').

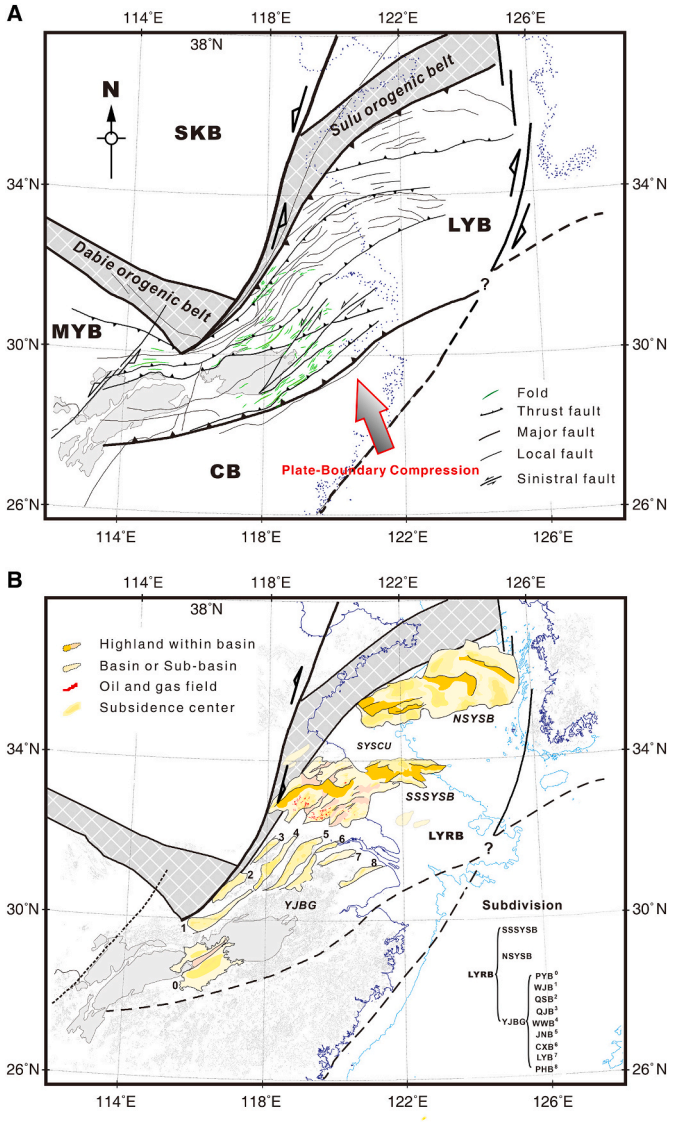

Fig. 7. (A) General basement framework and (B) extensional basin provinces in the Lower Yangtze region. The structure and pattern of the basin system are defined by its depocenter arrangement and the basin-bounding, syn-depositional faults. Abbreviation of the blocks, basins, and orogenic belts are similar to the Fig. 1. The geometry and architecture of the extensional basins onshore is established by the topographic and stratigraphic indicators, including the Poyang, Wangjian, Qianshan, Wuwei, Jurong-Nanling, Changzhou-Xuancheng, Liyang and Pinghu basins, labelled from 0 to 8 and abbreviated as follows, respectively: PYB, WJB, QSB, WWB, JNB, CXB, LYB, and PHB.

4. Extensional tectonics and basins in the Lower Yangtze block

4.1. Extensional structures and sedimentary observation

The Late Cretaceous-Paleogene extensional province in the Lower Yangtze block extends from the Korean Peninsula border westward to the TLFZ (Fig. 7B). Widespread extension in the Lower Yangtze region, following strong crustal shortening and left-slip faulting in response to the collision between the Sino-Korea and South China blocks, is evidenced by various-scale extensional basins, together comprising the giant basin system (Fig. 7B). Some basins, including the Subei-Southern South Yellow Sea and Northern South Yellow Sea basins, are relatively well preserved with thick Late Cenozoic sediments, whereas others like the Yan Jiang basin group are either uplifted or have been reworked by erosion (Fig. 8). Geographically, this basin province can be subdivided into three sub-provinces: the Yanjiang basin group, Subei-South Yellow Sea basin and Northern South Yellow Sea basin (Xu and Gao, 2015a; Xu et al., 2015b). The Yanjiang basin group contains nine NE-NEE-oriented individual basins—namely the Poyang, Wangjian, Qianshan, Wuwei, Jurong-Nanling, Changzhou-Xuancheng, Liyang and Pinghu basins—which are generally asymmetric basins bounded by a series of NE-NEE-striking normal faults (Xu et al., 2018). The Poyang basin, which topographically separates the Jiangnan-Jiulin orogenic belt, is a lacustrine intermontane basin that overlies the crystalline-metamorphic basement of the belt. The latter includes southern and northern portions, called the Subei-Southern South Yellow Sea basin and the Northern South Yellow Sea basin, respectively. They are divided by a structural uplift and basement highland composed of Meso-Paleozoic and Proterozoic metamorphic rocks, and termed the South Yellow Sea Central Uplift (e.g., Pang et al., 2018) (Fig. 7B). These basins are probably composed of over 30 sub-basins and 17 intra-basinal highlands, usually bounded by through-going normal faults. The syn-extensional strata tilted in the hanging walls, and thicken and coarsen toward major boundary faults (sub-basin-bounding or basin-bounding fault), which is indicated by the wedged syn-tectonic sequences within the half or asymmetric grabens (Fig. 9 and Fig. 10).

The Gaoyou sub-basin and Northern South Yellow Sea basin display a large majority of the basinal features shared by other synchronous sub-basins or basins in the Lower Yangtze region, of which the structural and depositional frameworks are well constrained by extensive seismic sections and boreholes, particularly in the northern South Yellow Sea (Fig. 11 and Fig. 12). The Gaoyou sub-basin with a single depocenter is bounded by the NE-striking Zhengwu and Wubao faults that exhibit a curvilinear trace, and displays half-graben geometry, and received sediments from its highlands (Fig. 11). As observed in some interpreted seismic profiles, the late Cretaceous-Paleogene sedimentation with a thickness of rarely over 3.5 km was clearly governed by normal faulting, although the strata and fault were buried beneath Neogene-Quaternary sediments. A dextral slip component is also observed on its NNE-striking fault segments (Fig. 11A). The NEE-elongated North South Yellow Sea basin was also predominantly fed by late Cretaceous-Paleogene detrital sediments, and the basin is characterized by various half-graben or graben geometries. The basin is bounded to the south by the Sulu orogenic belt, which appears to merge with the TLFZ to the southwest. The interpreted seismic sections reveal features of the basin-bounding faults and sedimentations (Fig. 11B). The sub-basins are bounded by a series of NEE-to-E-striking normal faults, separated from each other by a set of basement highs and covered by almost undeformed Neocene and Quaternary sediments, whose location is probably controlled by Mesozoic structural inheritance due to the Sino-Korea-South China block collision (e.g., Gao et al., 2015). The sub-basin-bounding faults are predominately normal faults, without any observed strike-slip component.

Constrained by the magnitude of well-imaged tectonic subsidence and normal faulting activity (Fig. 12) and a well-dated sedimentary unconformity (Fig. 2) (Zhu et al., 2010), Cenozoic extension of Northern South Yellow Sea basin is characterized by two phases (Fig. 2): (1) a fast extension stage with high extensional rates on the major boundary faults during the Late Cretaceous and Palaeocene (~0.1-0.6 km/Ma), followed by (2) slower extension from the Eocene to Oligocene (rates <0.1 km/Ma) (Fig. 12), which is similar in extensional evolution of the nearby Jianghan basin (Wu et al., 2018a) (Fig. 2). The maximum thickness of the Upper Cretaceous-Lower Paleogene strata is up to 4000 m in the northern portion of the Northern South Yellow Sea basin. The depocenter is close to the southern boundary of Sulu orogenic belt.

4.2. Extensional tectonics in the LYR

As revealed by the detailed basin geometry mapping and distribution shown in Fig. 13, the structural framework of the Lower Yangtze region is characterized predominately by normal faulting, which has partially

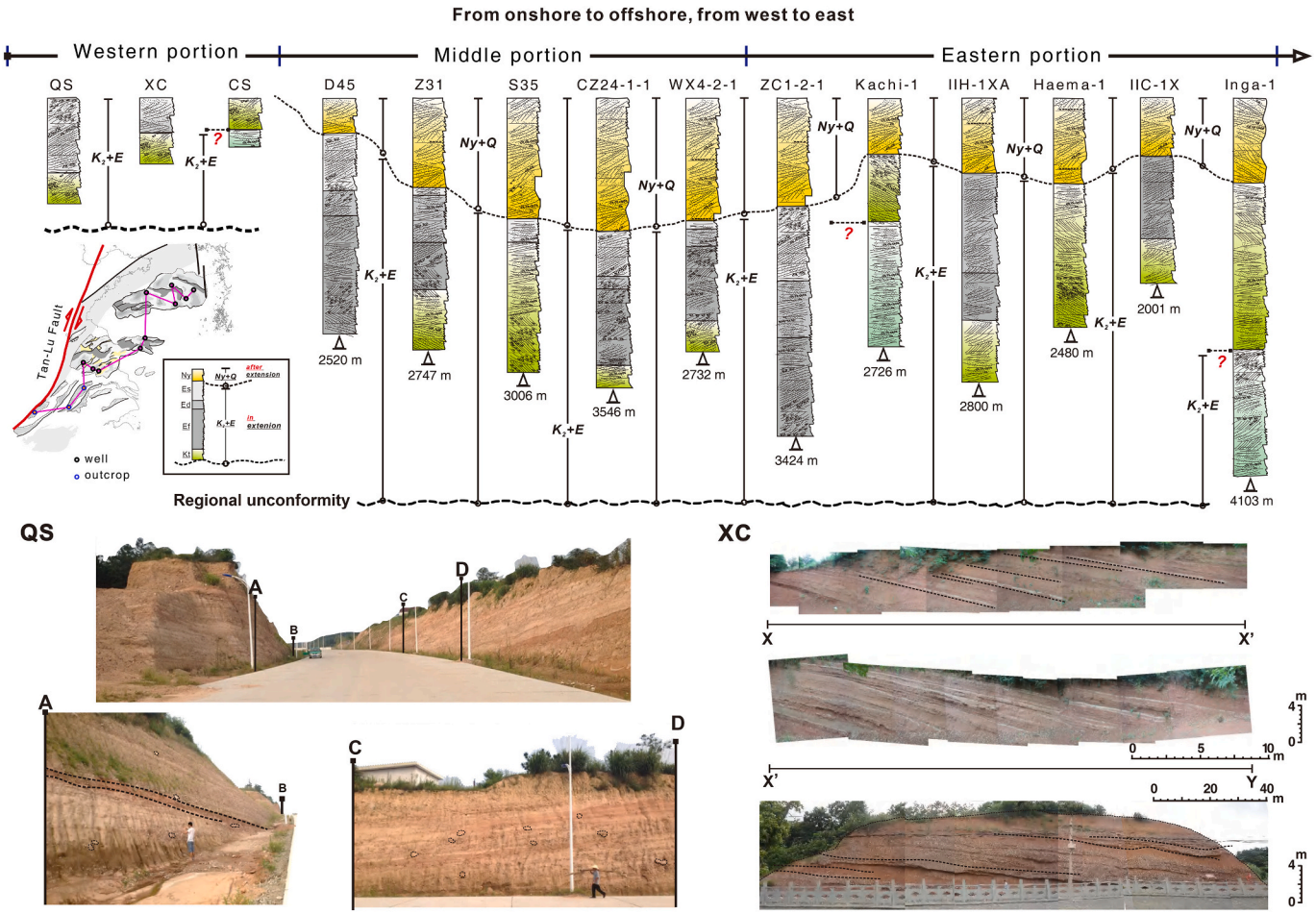

Fig. 8. Stratigraphic columns and framework of the Late Cretaceous-Cenozoic in the Lower Yangtze region basin (LYRB). Data for stratigraphic columns of the western portion of the LYB (Yanjiang Basin Group) are from our field investigation and the literature (AHBGMR (Anhui Bureau of Geology and Mineral Resources), 1987; JSBGMR (Jiangsu Bureau of Geology and Mineral Resources), 1987). Eleven selected wells from D45 to Inga-1 (from onshore to offshore), showing the syn-rift and post-rift strata. Syn-rift strata is exposed well in the Qianshan (QS) and Xuancheng (XC).

been superimposed by a relatively weaker component of strike-slip faulting, indicated by the presence of individual elongated basins. Based on variations of basin geometry and orientation, the basins and sub-basins can be regionally separated into three extensional tectonic domains from north to south, from onshore to offshore, exhibiting ribbon-like shapes in map view (Fig. 13). These are the Northern South Yellow Sea basin, the Subei-Southern South Yellow Sea basin, and the Yanjiang basin group, which are likely distributed over the pre-existing Mesozoic structure fabrics (Fig. 13). The Yanjiang basin group domain is mainly marked by NE-NEE-striking basins bordered by parallel normal faults. The Subei-Southern South Yellow Sea basin domain is typified by isolated basins with boundary faults striking from NE in the west to NEE-EW in the east (Fig. 13) (e.g., Xu and Gao, 2015a; Xu et al., 2015b; Gao et al., 2015). The Northern South Yellow Sea basin domain is dominated by nearly NEE-striking faults close to the Sulu orogenic belt. In the Yanjiang basin group and Northern South Yellow Sea basin, structural deformation indicates primarily dip-slip normal faulting with almost no strike-slip component. In the Subei-Southern South Yellow Sea basin, the key faults close to the sharp bend of the Sulu orogenic belt and the NNE-striking portion of the TLFZ, especially in the Jinhu and Gaoyou sub-basins (Fig. 13), exhibit normal faulting with a strong dextral slip component. Thus, the occurrence of an oblique strike-slip component in the basin-bounding normal faults depends on the orientation and spatial position of the fault structures relative to the NNE-striking portion of the TLFZ. Regionally, the strike of major boundary faults within the Lower Yangtze region is uniformly subparallel to the structural orientation of the Sulu orogenic belt offset and dragged by the Mesozoic sinistral slip along the TLFZ, varying from NNE in the west to NEE in the east (Fig. 13).

The fault-bounded basins occurred over a vast area with pre-existing Mesozoic faults. The geometry and localization of extensional deformation and resultant basins are strongly governed by the orientation of crustal inherited basement fabric, indicating that the extensional tectonics could be intrinsically related to the Sino-Korea-South China block collision and the TLFZ strike-slip movement. An exception is the NW-W-striking depression-bounding faults and related uplifts in the eastern segment of the Northern South Yellow Sea basin (Shinn et al., 2010). Additionally, comparison of the Pre-Cretaceous and Cenozoic structural frameworks across the Lower Yangtze region reveals that the normal faults and these related underlying Pre-Cretaceous ancient faults have consistent strikes and inheritance (Fig. 7). Deduced from the Late Triassic rotation collision (i.e., Indosinian) between the Sino-Korea and Lower Yangtze blocks (Chang and Zhao, 2012), the local basement framework and pre-existing weak zone beneath the Qunsan sub-basin made local structures more complex.

5. Tectonically coupled deformation between Bohai Bay and the Lower Yangtze basin

5.1. Cenozoic evolution of the Tan-Lu Fault Zone

The ~2,400-km-long NNE-striking Tan-Lu fault zone is the first-

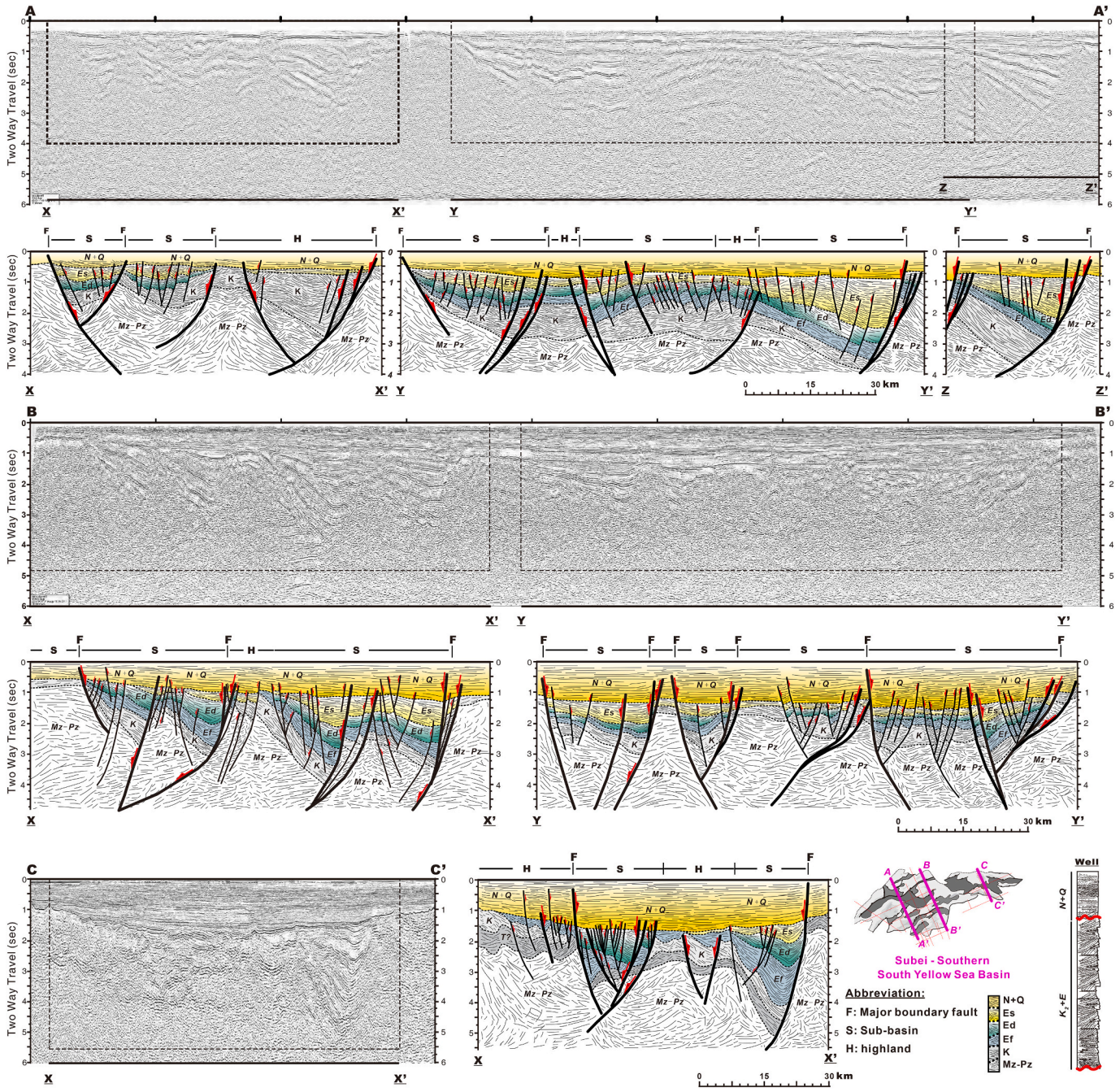

Fig. 9. Uninterpreted and interpreted seismic sections AA', BB' and CC' across the Subei-Southern Yellow Sea Basin, showing the syn-rift and post-rift strata and related boundary faults. Note that major boundary faults with high angle bounds half-graben or graben sub-basins. Location of sections is shown in inset map. Vertical axis is in two-way travel time (seconds).

order regional strike-slip fault system in east China (Fig. 1A). This subvertical lithosphere-scale fault zone, which produces earthquakes at depths of up to nearly 100 km (e.g., Hsiao et al., 2004, 2010; Chen et al., 2006; Zheng et al., 2008), has been active during several phases since the Mesozoic, as constrained by geological, geophysical, and geochronological data (Yin and Nie, 1993; Zhu et al., 2009a; Zhu et al., 2018). The fault is interpreted as the primary tectonic boundary between the Sino-Korea block to its west and the Lower Yangtze block to its east (Chen et al., 2006; Huang et al., 2015; Zhao et al., 2016). It is widely accepted that the TLFZ formed during the Late Triassic-Jurassic Sino--Korea-Lower Yangtze block collision and acted as a left-slip ductile shear zone (e.g., Xu et al., 1987; Yin and Nie, 1993; Gilder et al., 1999; Zhu et al., 2005, 2009a, 2009b), whereas it experienced right-slip motion during the Cenozoic (e.g., Allen et al., 1997, 1998; Hsiao et al., 2004). Estimates of the magnitude of Mesozoic left-slip displacement of several 100s km is far greater than Cenozoic left-slip displacement on the order of 10s of km (Huang et al., 2015). The Mesozoic sinistral deformation history is relatively well documented, but Cenozoic dextral motion is poorly constrained due to limited Cenozoic strata preserved in outcrops along the onshore TLFZ. However, Cenozoic strata in the Bohai Bay basin are relatively well constrained, thus providing the best records of right-slip fault activity (e.g., Hsiao et al., 2004; Huang et al., 2012; Huang et al., 2015, 2018).

As revealed by exploration-based seismic data from the Bohai Bay basin, the structural relationship between TLFZ-related vertical strike-slip faults and listric normal faults shows that these TLFZ-related

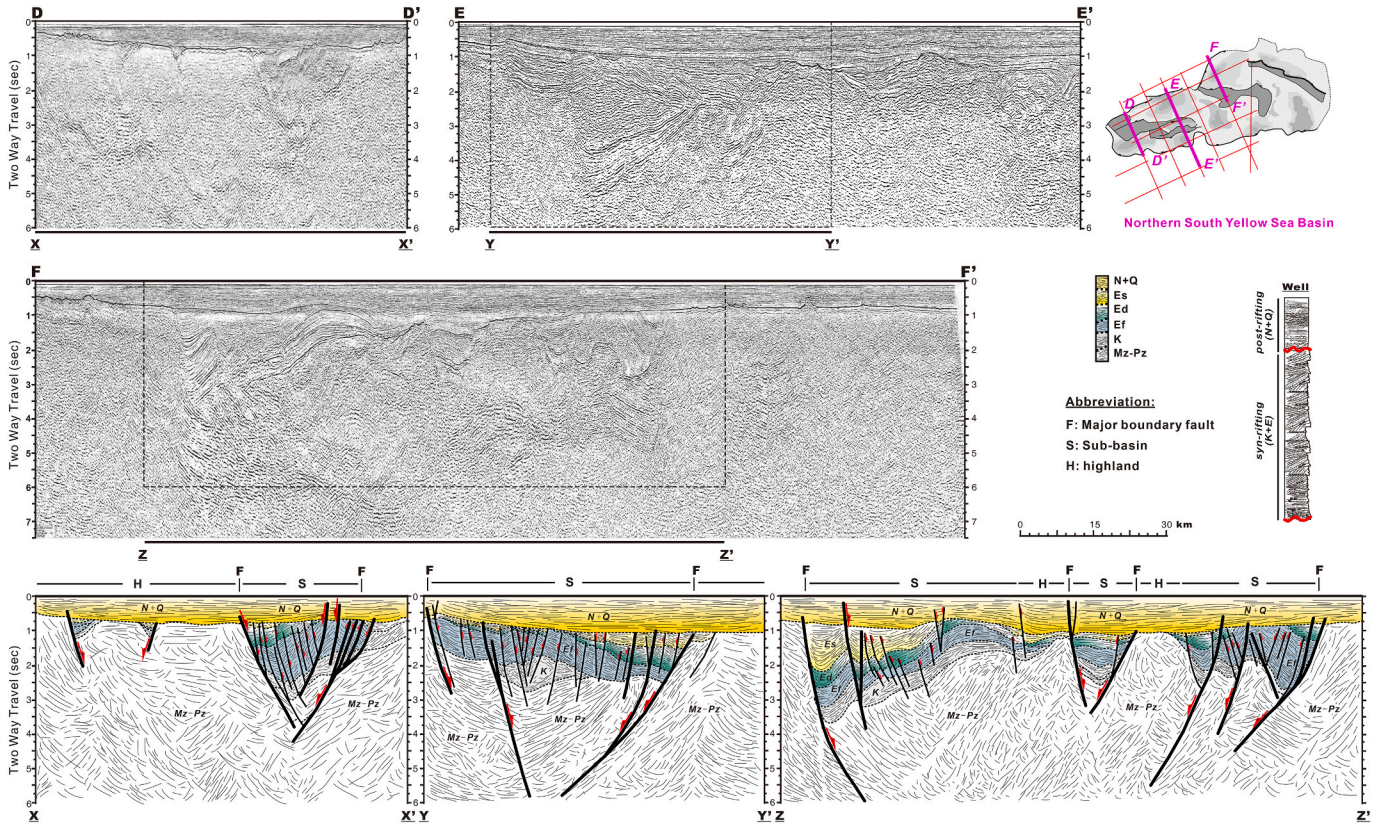

Fig. 10. Uninterpreted and interpreted seismic sections DD', EE' and FF' across the Northern Southern Yellow Sea Basin, showing the syn-rift and post-rift strata and related boundary faults. Note that major boundary faults with high angle bounds half-graben or graben sub-basins. Location of sections is shown in inset map. Vertical axis is in two-way travel time (seconds).

strike-slip faults controlled the development of Paleogene half-grabens (e.g., Qi and Yang, 2010) and acted as the half-graben listric boundary faults terminating near the bottom of the ca. 40 Ma Shahejie Formation (E_2s^2) (Qi and Yang, 2010; Huang et al., 2015). This implies that the Cenozoic tectonic regime of the TLFZ transformed from extensional deformation to right-slip at ca. 40 Ma. Additionally, depositional observations indicate that the TLFZ experienced weak sinistral motion before ca. 40 Ma (Han et al., 2005; Cao, 2008; Xu et al., 2008b). Furthermore, bends in the fault trend that are expressed in Cenozoic strata are well identified along the TLFZ in Bohai Bay basin, providing direct evidence for dextral motion along the fault, with most of the bends forming after the deposition of Shahejie Formation (E_2s^2) strata (ca. 40 Ma) during the deposition of the Shahejie-Dongying (E_2s^2-E_3d) Formation (ca. 38-25 Ma) (Huang et al., 2015). Notably, during the Neogene and Quaternary, most of these fault bends were enhanced and TLFZ-related minor faults formed in en echelon pattern (Zhu et al., 2009a; Gong et al., 2010; Huang and Liu, 2014; Huang et al., 2015), indicating the TLFZ continuously deformed dextrally. Moreover, the Neogene-Quaternary strata record reveals that these TLFZ-related subsidiary faults are formed after 12 Ma and become progressively more abundant crosscutting shallower strata (Zhu et al., 2009a; Gong et al., 2010; Huang et al., 2012), finally reaching maximum dextral slip after ca. 5 Ma (Huang and Liu, 2014; Huang et al., 2015). Evidenced by present-day seismicity (Chen and Nábelek, 1988; Hsiao et al., 2004) and GPS measurements (Xie et al., 2004; Xu et al., 2008c) the fault is still active today, and therefore its dextral slip has been ongoing since ca. 40 Ma to the present.

In summary, the Cenozoic evolution of the TLFZ includes two distinct stages (Fig. 2) (e.g., Huang et al., 2015): (1) extensional deformation from 65 to 40 Ma (with a possible weak sinistral shear sense) and (2) dextral movement from 40 Ma to present, with the most intense dextral movement from 40 to 25 Ma, an anticlockwise change of dextral direction from nearly NE-SW to N-S trends at 25 Ma, enhanced motion after 12 Ma, and accelerated deformation after 5 Ma. However, the first-order driving mechanism for Cenozoic dextral strike-slip movement of the TLFZ remains debated, with main end-member models involving the westward subduction of the (Paleo-) Pacific plate beneath the Eurasia plate (e.g., Allen et al., 1997, 1998; Qi and Yang, 2010) or extrusion tectonics related to the India-Asia collision (e.g., Molnar and Atwater, 1978; Kimura and Tamaki, 1986). These transitions imply a complicated modulation of deformation by the two plate-boundary conditions along the eastern and southern margins of the Asian continent. India-Asia collision initiated at ca. 58 Ma (e.g., DeCelles et al., 2014; Hu et al., 2015, 2016) and contractional deformation extended across much of Tibet by the Eocene (Yin et al., 2008; Cheng et al., 2019; An et al., 2020; Li, 2020; Wang et al., 2021). Related to a combination of Indian slab dynamics, tearing, and Asian crustal thickening, the Tibetan crust started to extend eastward via a combination of strike-slip and normal faulting at ca. 20-10 Ma (e.g., Molnar et al., 1993; Yin et al., 1999; Styron et al., 2015; Zuza and Yin, 2016; Webb et al., 2017; Bian et al., 2020). During India-Asia collision and continued convergence, collision-related stress propagated to the eastern Tibetan Plateau, evidenced by the observations that notable exhumation initiated at ~12-10 Ma and continued to present (Ouimet et al., 2010; Tian et al., 2015), which might have enhanced TLFZ dextral motion since 12 Ma (Fig. 2).

It has been previously proposed that variations in the direction and velocity of the (Paleo-) Pacific subduction revealed by the spatial-temporal framework of the Hawaiian-Emperor bend and seamount trail may directly drive the dextral movement of the TLFZ at ca. 40 Ma (e.g., Huang et al., 2015, 2018; Zhu et al., 2012). However, new published geochronology results date the Hawaiian-Emperor bend at ca. 49.4 Ma, and the crucial Pacific plate motion to 25.3 Ma, which modifies

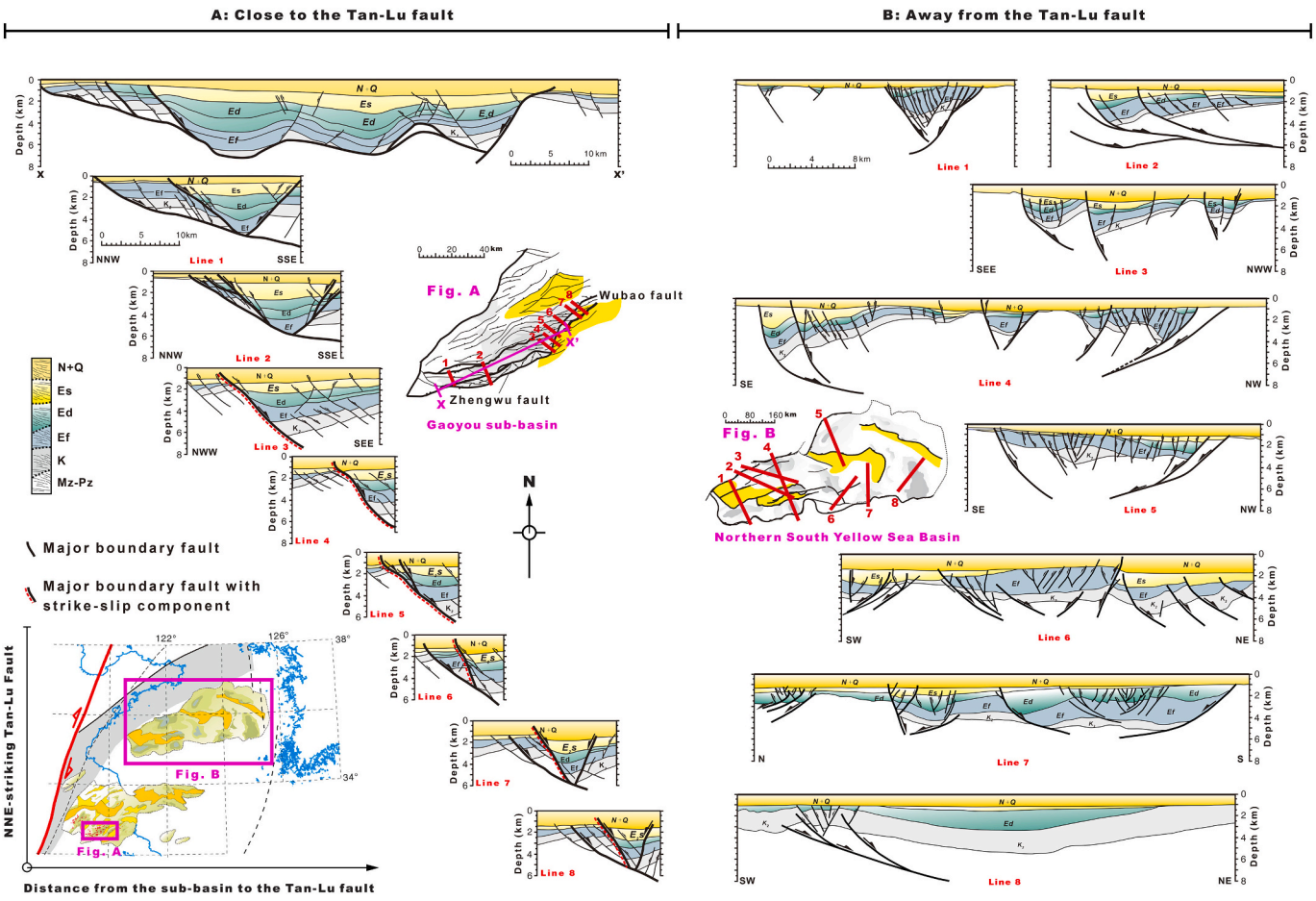

Fig. 11. Structural cross-sections intersecting the major boundary faults within the Gaoyou sub-basin and NSYSB located close to (A) and away from (B) the Tan-Lu fault, respectively, which could be divided into two categories: NNE-striking normal fault with strike-slip component and normal fault, respectively. Locations of geological sections in map A, numbered from 1 to 8 and labelled XX', complied and modified from Jiang (2013). All the sections in Fig. 11B are interpreted from 2D seismic data, except of the sections labelled from 6 to 8 (Shinn et al., 2010).

the timing of mid-Cenozoic counter-clockwise rotation of the Pacific plate (Jicha et al., 2018). Recent geological observations and numerical modelling reveal that East China experienced subduction of Paleocene Izanagi plate, Eocene Izanagi-Pacific mid-ocean ridge, and Miocene Pacific plate during the Cenozoic (Whittaker et al., 2007; Müller et al., 2016; Wu and Wu, 2019), which may be alternative drivers for the Cenozoic evolution of the TLFZ.

5.2. Structure and evolution of the Bohai Bay and Lower Yangtze basins

Located in the thinnest portion of Sino-Korea block with maximum amount of crustal thinning, the Bohai Bay basin is a Cenozoic intracontinental rift basin characterized by a rotated-"Z" shape (Fig. 1A) and underlain by an Early Cretaceous-Late Jurassic sedimentary basement (e.g., Qi and Yang, 2010; Liu et al., 2017a, 2017b). Bohai Bay evolved during two main stages: 1) Paleogene (ca. 65-25 Ma) syn-rifting and 2) Neogene-Quaternary (ca. 25-0 Ma) post-rifting subsidence (Fig. 2) (Zhu et al., 2009b; Huang et al., 2012; Qi and Yang, 2010; Li et al., 2012a, 2012b). During the Paleogene, this basin formed by intracontinental rifting with rapid tectonic subsidence and volcanism (Hsiao et al., 2004; Huang et al., 2012). At least 7-km-thick Cenozoic strata accumulated in faulted subbasins, which are all bounded by normal faults and local strike-slip faults. Followed by diminished faulting and post-rifting thermal subsidence, these Paleogene faulted subbasins were buried by Neogene-Quaternary strata (Hsiao et al., 2004; Huang et al., 2012; Qi and Yang, 2010). During the Cenozoic, the Bohai Bay basin was filled with syn-rift strata (ca. 60-25 Ma) including the Kongdian, Shaheji, and Dongying Formations and post-rift strata (ca. 25-0 Ma) of the Guantao, Minghuazhen and Pingyuan Formations (Fig. 2) (Zhu et al., 2009b; Huang et al., 2012; Qi and Yang, 2010; Li et al., 2012a, 2012b).

The TLFZ bounds the Bohai Bay basin to its east, and due to its accommodation of 100s of km of strike-slip displacement in the Mesozoic (e.g., Xu and Zhu, 1994), this fault was presumably a pre-existing tectonic weak zone prior to the Cenozoic. Its spatial location along the eastern flanks of the Bohai Bay extensional basin suggests that the TLFZ-related strike-slip faulting strongly offset and/or deformed the extensional rift structures, especially where the TLFZ extends axially through the center of a faulted subbasin (e.g., Hsiao et al., 2004; Huang et al., 2015, 2018). Superimposed by TLFZ-related strike-slip structures, the extensional structures of offshore basin is more complex than that of onshore basin (Qi and Yang, 2010; Huang et al., 2015, 2018). Facilitated by high-quality seismic reflection data derived from petroleum exploration, seismically well-imaged TLFZ and basin structures reveal that the TLFZ apparently interacted with rifting deformation and partitioned the strain since the Late Eocene (ca. 40 Ma), deepening and shallowing the local areas with transtensional and transpressional tectonism, respectively (e.g., Hsiao et al., 2004; Qi and Yang, 2010).

Well-constrained seismic datasets demonstrate that the Bohai Bay basin is dominated by two relatively independent structural deformation systems (Waldron, 2005; Qi and Yang, 2010): (1) Paleocene-Late Oligocene dip-slip normal faulting and (2) Oligocene-Miocene dextral faulting, which generated eleven extensional and three strike-slip systems (Qi and Yang, 2010). Most importantly, high-quality seismic sections and drill cores reveal that the Bohai Bay basin experienced at least

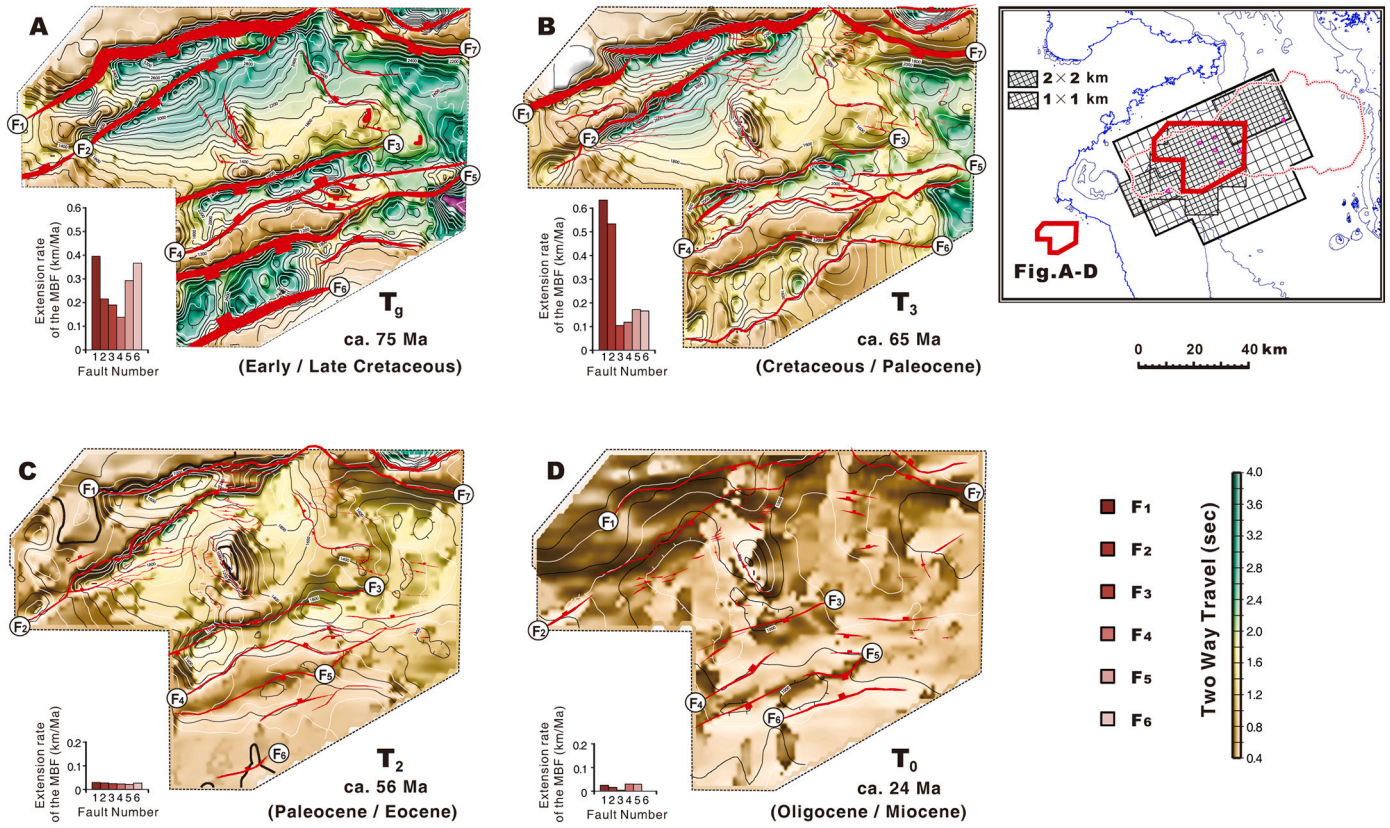

Fig. 12. Maps, labelled from A to D, showing the distribution of faults and subsidence in the contour maps of sedimentary unconformity T_g (ca. 75 Ma, Early/Late Cretaceous), T_3 (ca. 65 Ma, Cretaceous/Paleocene), T_2 (ca. 56 Ma, Paleocene/Eocene), and T_0 (ca. ~24 Ma, Oligocene/Miocene), respectively, which are interpreted from high-resolution 2D seismic dataset with line spacing of 1 km × 1 km and 2 km ×2 km. The extension rate on the major boundary faults, typified by the fault numbered from No.1 to No.6, indicate the magnitude of faulting activity.

six rifting episodes expressed by multiple regional unconformities (Fig. 2) (Huang et al., 2012): (1) Eocene Kongdian and Shahejie Formations (E_2k/E_2s^4 unconformity; ca. 50 Ma), (2) Eocene Shahejie-Member-4 and Shahejie-Member-3 Formations (E_2s^4/E_2s^3 unconformity; ca. 42 Ma), (3) Eocene Shahejie-Member-3 and Shahejie-Member-2 Formations (E_2s^3/E_2s^2 unconformity; ca. 38 Ma), (4) Eocene Shahejie-Member-1 and Oligocene Dongying Formation (E_2s^1/E_3d unconformity; ca. 32.8 Ma), (5) Oligocene Dongying and Miocene Guantao Formation (Paleogene unconformity; ca. 24 Ma), and (6) Pliocene and Quarternary (Pliocene unconformity; ca. 5.1 Ma). Furthermore, evidenced by the onshore-offshore migration of depocenter and subsidence centers, the spatial variation in sedimentary strata distribution, and the structure and activity of the rift-related faulting, it is notable that the Late Eocene-Early Oligocene (ca. 40-38 Ma) and Late Oligocene-Early Miocene (ca. 24-25 Ma) unconformities are both regional uplift events that impacted the entire basin, whereas the rest are all the records of local deformation at the edge of the basin or subbasin (Huang et al., 2012, 2015, 2018; Huang and Liu, 2014). The former are recognized as two key tectonic points of regionally dynamic transition, and the latter could be closely related to local tectonic transitions.

Although the Lower Yangtze basin is also located at the similar tectonic location in the back-arc region during subduction and rollback of the Pacific oceanic slab, it has a more complex sedimentary framework (Figs. 1 and 2). Late Eocene and Oligocene sediments are mostly absent, presumably due to tectonic uplift, while the Bohai Bay basin filled with Late Eocene-Oligocene strata (Fig. 2). Furthermore, there is a regional angular unconformity between the Paleocene and Eocene strata within the extensional basins across East China, except of the Bohai Bay basin (Fig. 2). These discrepancies based on updated observations demonstrate that the kinematics and evolution of the Cenozoic extensional tectonics in east China are more complex than that previously thought. Existing model oversimplify these kinematics, including models that invoke back-arc or slab window influences from the Cenozoic (Paleo-) Pacific subduction (Ren et al., 2002; Mercier et al., 2007, 2013a, 2013b; Yin, 2010) or a change in the subduction direction of the Pacific plate (Qi and Yang, 2010; Huang et al., 2015, 2018). Therefore, an updated regional tectonic model of the TLFZ, compatible with all these observations, is necessary.

We start with knowledge that the Cenozoic succeeding subduction of the Izanagi plate, the Izanagi-Pacific mid-ocean ridge, and Pacific plate (Whittaker et al., 2007; Müller et al., 2016) provide independent time-space constraints on the Pacific margin here. Wu and Wu (2019) observed a 56-46 Ma magmatic gap along the northeast Asian margin from a widespread compilation of Mesozoic and Cenozoic igneous samples, which they interpreted to result from subduction of the Izanagi-Pacific mid-ocean ridge. Furthermore, their study provided temporal-spatial constraints for the location of the Izanagi-Pacific mid-ocean ridge in the early Cenozoic. Moreover, the newest $^{40}Ar/^{39}Ar$ dating for lavas spanning the entire Northwest Hawaiian Seamount trails re-constrained the previously accepted time of the Hawaiian-Emperor bend, proposing an important 25.3-Ma kink in the Hawaiian trails and a newly-estimated velocity range of the Cenozoic Pacific plate (Jicha et al., 2018). The new observations help us to provide a new evolution history of the Izanagi-Pacific Plate during the Cenozoic to compare with structural and sedimentological records in eastern China (Wu and Wu, 2019; Jicha et al., 2018; Wu et al., 2018a; Xu and Gao, 2015a; Qi and Yang, 2010) (Fig. 2).

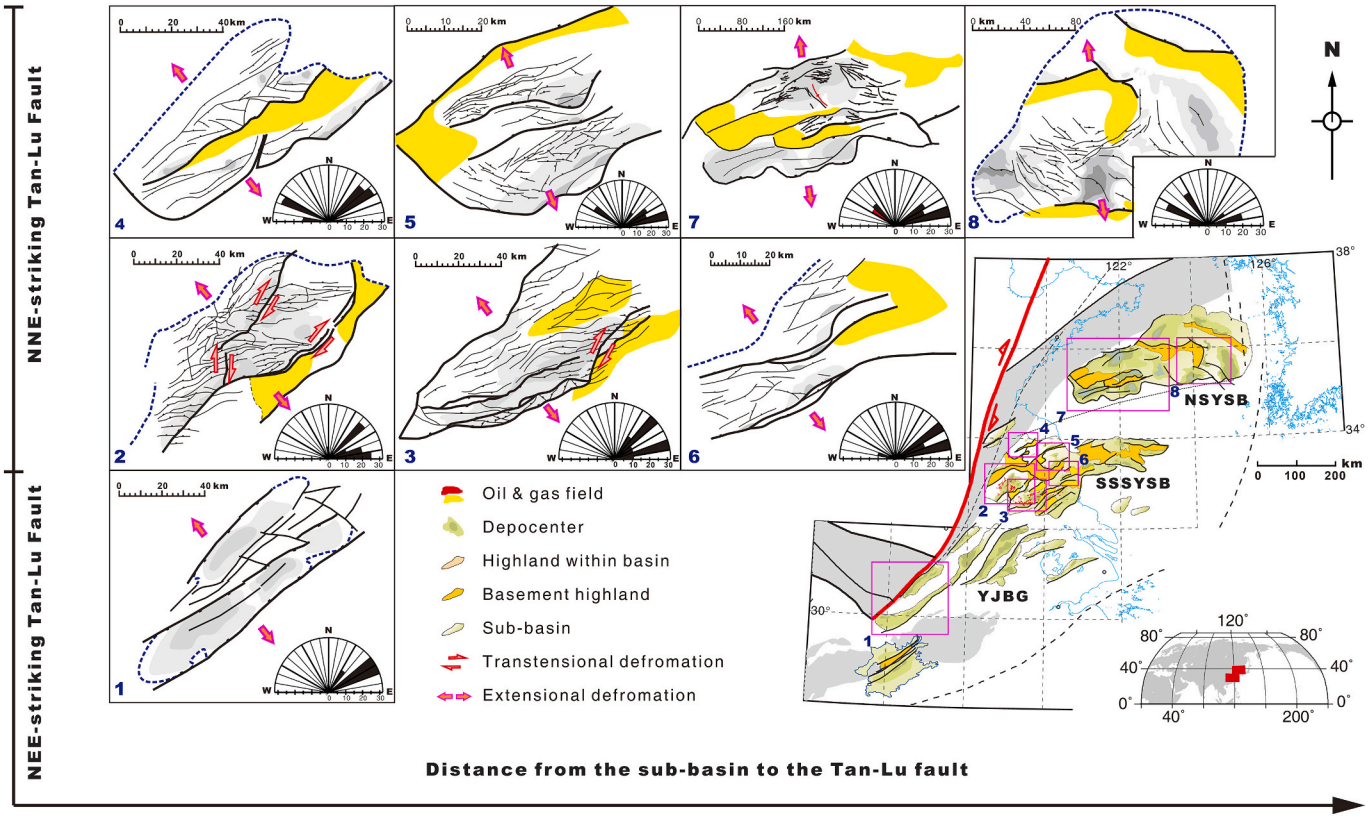

Fig. 13. Distribution of faults offsetting rift strata and related structure stress within major sub-basins. Locations of the basin and sub-basin are in inset map. The major representative basins and sub-basins labelled from 1 to 9, successively corresponding to the Wangjiang-Qianshan basin, Jinhu sub-basin, Gaoyou sub-basin, Lianshui sub-basin, Yancheng sub-basin, Baiju sub-basin, eastern of NSYSB sub-basin, and western of NSYSB sub-basin (Qunshan sub-basin).

5.3. An updated kinematic model for coupled Cenozoic Bohai Bay-Lower Yangtze deformation

Extensive Mesozoic magmatism is widely distributed across eastern China (e.g., Charles et al., 2013; Li et al., 2014; Liu et al., 2019; Wu et al., 2019). There is a westward younging trend in the Jurassic (200-145 Ma) and eastward younging trend in the Cretaceous (145-100 Ma), which has been interpreted to reflect flattening of Mesozoic Izanagi-slab subduction (e.g., Liu et al., 2013, 2018; Liu et al., 2019; Wu et al., 2019), followed by continuing subduction of the Izanagi-Pacific ridge and Pacific plate during the Cenozoic (e.g., Liu et al., 2017a; Müller et al., 2019; Wu and Wu, 2019; Liu et al., 2021d). Consequently, the spatial extent of Mesozoic magmatism may outline the area most directly impacted by oceanic slab rollback and characterized by weakened and thinned lithosphere, which is spatially correlated with the Cenozoic tectonic evolution of Bohai Bay-Lower Yangtze region (e.g., Liu et al., 2021a) (Figs. 1 and 4). Before Early Cenozoic ridge subduction (65-56 Ma), the nested sedimentary basins of eastern China within and around the TLFZ were all extending contemporaneously (Figs. 2 and 14A), implying that there was a stable dynamic setting for regional extensional that likely corresponded to the eastward rollback phase of the Izanagi plate. When the Izanagi-Pacific mid-ocean ridge started to subduct beneath the nearby trench at ca 56 Ma, evidenced by a near-synchronous 56-46 Ma magmatic gap along strike of the arc (Wu and Wu, 2019), the predicted compressional stress originated from the plate boundary transmitted to the continental interior, evidenced by a coeval regional unconformity in these syn-rift basins east of the TLFZ, including the Jianghan, Lower Yangtze, and Northern East China Sea (Changjiang depression) basins (Fig. 2) (e.g., Wu et al., 2018a; Xu and Gao, 2015a; Zhu et al., 2009a, 2009b). As evidenced by the relatively continuous sedimentary sequence (Fig. 2), the Bohai Bay basin was not significantly deformed, indicating that the bounding TLFZ may have acted as a strain partitioning zone to accommodate stress transmitted from the plate boundary (Fig. 14B). That is, the TLFZ allowed the Bohai Bay block to remain stable with deformation partitioned around it. Along with the Early Eocene syn-rifting subsidence, there is a pronounced ca. 50 Ma sedimentary unconformity recorded in the Bohai Bay and Jianghan basins (Fig. 2 and Fig. 14B). Of note, inferred ridge subduction at ca. 50 Ma is approximately coeval with the Hawaiian-Emperor bend in the Pacific plate (49.4 Ma; Jicha et al., 2018), which may reflect reorganization of Pacific plate motion (e.g., O'Connor et al., 2013). However, it is impossible to completely deconvolve Pacific-related uplift in eastern China due to Pacific ridge subduction and collisional tectonics associated with the India-Asia collision (e.g., Lee and Lawver, 1995; Yin and Harrison, 2000; Yin, 2010; Van Hinsbergen et al., 2012; Kapp and DeCelles, 2019), which may have affected eastern China in the far field.

During the Late Eocene and Oligocene, the coupled structure-sedimentary records reveal a complex tectonic setting in East China (Fig. 2). For example, while the East China Sea and Jianghan basins accommodated extension during this time, the Bohai Bay and Lower Yangtze region basins experienced transtension and intense erosion, respectively, which may reflect a complex superposition result of multi-dynamic tectonic processes (Fig. 14B). Specifically, the dextral movement of these strike-slip faults across East China were likely driven by a regional compressional stress originated from east of basin province, evidenced by a gradual decrease from east to west in the size and continuity of the Tan-Lu strike-slip fault system within the Bohai Bay basin (Huang et al., 2015; Qi and Yang, 2010). The subduction direction of the Pacific plate varied from NWW to W at ca. 40 Ma (Müller et al., 2016), which could alternatively trigger the activation of dextral motion on the TLFZ. This transition was accompanied by a regional unconformity recorded within the nested sedimentary basins around the TLFZ (Fig. 2).

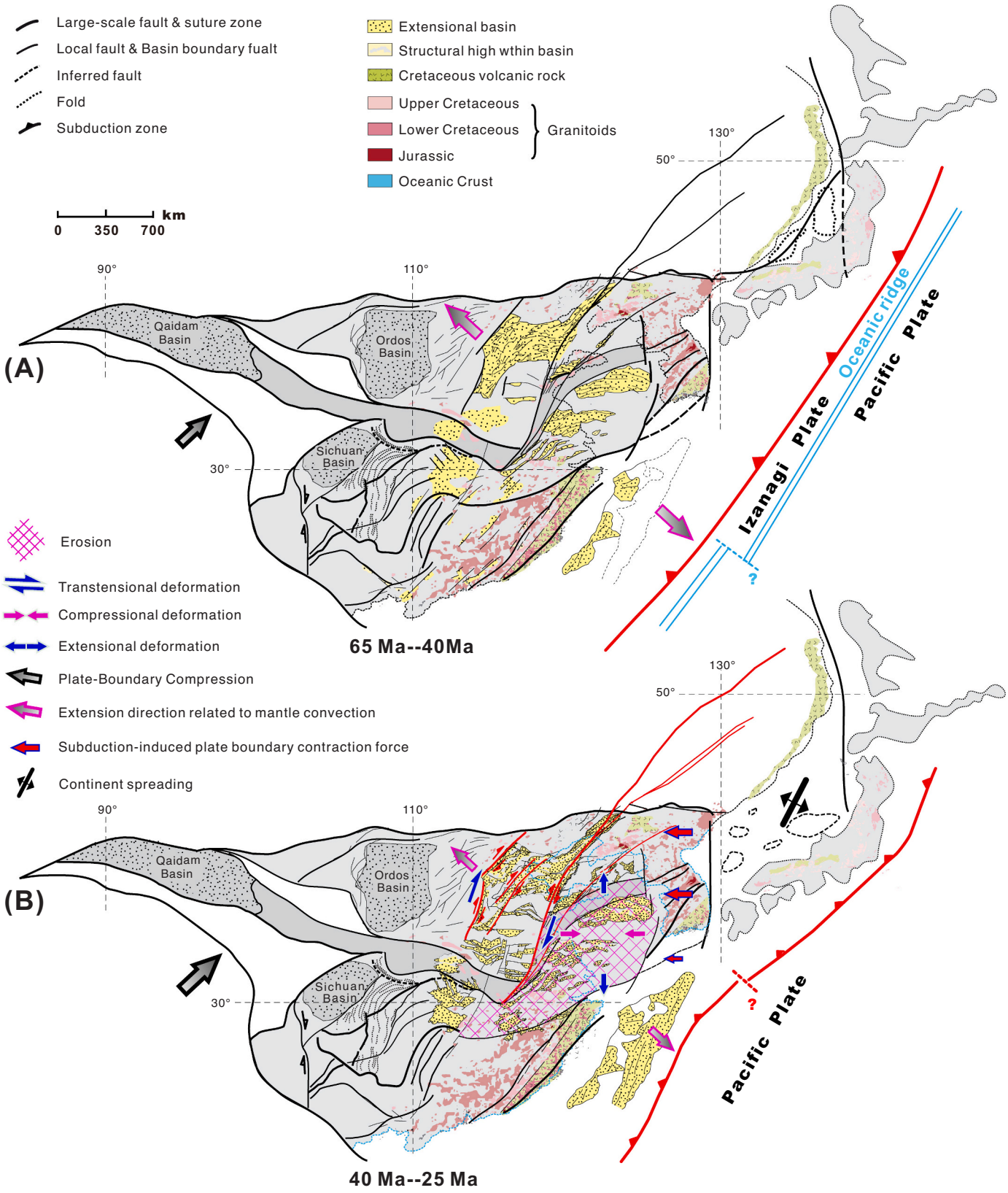

Fig. 14. Kinematic tectonic model of the East China during the Late Cretaceous-Paleogene, with two stages: (A) Late Cretaceous-Paleogene regional extension driven by Izanagi subduction-induced process, and (B) Eocene-Oligocene coupled deformation in the Lower Yangtze-Bohai Bay region driven by Pacific subduction-induced processes.

The ongoing Late Eocene-Oligocene westward subduction (ca. 40-25 Ma) drove the initial extension in the proto Japan Sea, continuous TLFZ dextral faulting, and uplift and erosion of the Lower Yangtze block. Meanwhile, within the Bohai Bay basin, a critical variation of structural regime also initiated at ca. 40 Ma, expressed as a composite structural mode of strike-slip and extension (Qi and Yang, 2010; Huang et al., 2012, 2015). Extensional deformation dominated the entire Bohai Bay basin during the Cenozoic, whereas the dextral strike-slip deformation initiated to activate in the Oligocene and exhibit locally in the TLFZ-related strike-slip faults, offsetting and/or deforming the extensional structures (Fig. 14B). Although other works have discussed this previously (e.g., Ren et al., 2002; Qi and Yang, 2010; Huang et al., 2015; Liu et al., 2017a), these studies have not focused on the kinematic linkage between the Late Paleogene dextral motion of the TLFZ and coupled Bohai Bay-Lower Yangtze extensional deformation. As a lithospheric-scale strike-slip fault zone, the TLFZ may effectively partition the tectonic stress transmitted from the Pacific plate boundary. Regionally and tectonically, its dextral strike-slip movement dominated the Bohai Bay basin as a transtensional regime (Qi and Yang, 2010), and coevally accommodated E-W crustal shortening in the Lower Yangtze block (Fig. 14).

6. Discussion

6.1. Slab age, subduction morphology, trench motion, and mantle wedge convection

Geological and geophysical data demonstrate that Pacific plate subduction beneath the Eurasia continent drives first-order deformation of the overriding East Asia lithospheric deformation, especially intra-plate extension (e.g., Northrup et al., 1995; Clark et al., 2008; Dal Zilio et al., 2018). However, exactly how intra-plate extension is dynamically coupled with oceanic subduction has long been debated (e.g., Ren et al., 2002; Yin, 2010; Liu et al., 2017a). Here, we interpret the integrated geological and geophysical dataset in the context of the known western Pacific subduction history. Our knowledge of Pacific subduction kinematics have improved substantially over the past decade due to improved geochronology and systematic numerical modelling (e.g., Müller et al., 2016; Yang et al., 2018a, 2018b), which allows for a refined understanding of the evolution of the Pacific plate (e.g., Jicha et al., 2018; Wu and Wu, 2019).

Subduction during the Mesozoic and Cenozoic involved oceanic plates that varied in age at the subduction trench. Consumption of the Izanagi oceanic plate at the trench gradually became younger during its subduction, as the oceanic lithosphere age decreased toward the mid-ocean ridge separating the Izanagi plate from the Pacific plate. Following subduction of the Izanagi-Pacific mid-ocean ridge, the subducting Pacific plate was gradually older at the trench (e.g., Whittaker et al., 2007; Müller et al., 2016; Wu and Wu, 2019). Global syntheses of subduction zones reveals no clear systematic correlation between slab age and subduction angle (Lallemand et al., 2005; Sdrolias and Müller, 2006; Garel et al., 2014; Goes et al., 2017). Review of global-scale tomography-Benioff seismicity imaging reveals how slab geometry, especially the style of slab and mantle transition zone interaction, is most dominantly driven by the trench mobility and its tendency to retreat (Goes et al., 2017). Trench mobility is controlled by deformation in the overriding upper plate, relative plate motion (Garel et al., 2014; Holt et al., 2015; Yang et al., 2018a, 2018b), and the strength and relative buoyancy of the subducting plate (Capitanio et al., 2007; Bellahsen et al., 2005; Tagawa et al., 2007; Ribe, 2010), which all relate to the age of the downgoing oceanic slab (e.g., Yang et al., 2018a, 2018b). Although trench mobility does not simply follow an age tendency (Sdrolias and Müller, 2006; Goes et al., 2011), old oceanic slabs tend to stagnate at the MTZ more often than young slabs (King et al., 2015). Thus, older, colder, and stronger plates are more capable of inducing trench retreat and slab stagnanation at the MTZ, whereas relatively young slabs more commonly penetrate the MTZ, as observed and modelled in West Pacific Plate subduction system (Goes et al., 2017; Yang et al., 2018a, 2018b).

There is a clear positive correlation between the age of the oceanic slab at the trench and increasing plate velocity (Carlson et al., 1983; Lallemand et al., 2005; Goes et al., 2011), interpreted as an expression of upper-mantle slab pull and driving force of the plate (Conrad and Lithgow-Bertelloni, 2002; Faccenna et al., 2007; Goes et al., 2011). The greatest trench-migration velocities generally occur for slabs older than ca. 50 Ma (e.g., Molnar and Atwater, 1978; Sdrolias and Müller, 2006; Goes et al., 2011), which then can impact slab morphology and dip (e.g., Yang et al., 2018a, 2018b).

In summary, the geometry of the subducting slab is related to trench migration kinematics (Goes et al., 2017), which are influenced by slab age. This is why back-arc spreading and stagnant slab tend to be associated with old oceanic slab subduction (Agrusta et al., 2017; Yang et al., 2018a, 2018b). Furthermore, unlike the subduction of younger slabs, older downgoing oceanic slabs ($>$ 50 Ma) generally induce sufficiently large force to overcome the forcing by upper plate or convective mantle that may impede trench motions, thus further providing a stronger driving force for mantle convection (Goes et al., 2017; Yang et al., 2018a, 2018b). We use these interpretations based on modelling results and global synthesis to hypothesize that subduction of older slabs tends to generate strong mantle-wedge convection, trench retreat, and upper plate extension, whereas subduction of younger oceanic slabs favors steeper subduction with weak mantle-wedge convection, and lower magnitude crustal extension.

6.2. Mechanism of intra-plate extension across the eastern China

Due to the complex temporal-spatial structural and geological observations from eastern China, models of relatively simple back-arc extension (e.g., Ren et al., 2002; Yin, 2010; Liu et al., 2017a) do not adequately explain the regional geological records. Instead we argue that the punctuated and variable kinematics of Cenozoic deformation in east China must reflect superposed tectonic processes. The extensional and strike-slip deformation in the basin province could have been induced by combined intraplate body forces, shear forces at the base of the lithosphere, and plate-edge forces (e.g., Sonder and Jones, 1999). Correspondingly, the driving force for intra-plate continental deformation is mainly governed by the competition between plate boundary forces driven by relative plate motion and basal traction driven by mantle convection and flow acting on the base of continental lithosphere (e.g., Ziegler and Cloetingh, 2004; Finzel et al., 2015). During the subduction and rollback of Izanagi-Pacific plate, forces related to inter-plate convergence or slab rollback and convecting mantle drag can interfere either constructively or destructively on the intracontinental lithosphere, thus contributing towards either extension or compression.

As presented above, the Sino-Korea and Lower Yangtze blocks are bounded by Pre-Cenozoic orogenic belts, floored by extensive Mesozoic compressional structural fabrics, and nested by series of Late Cretaceous-Cenozoic sedimentary basins. The Lower Yangtze region is distributed along the Sulu orogenic belt (Fig. 7). When Izanagi-Pacific subduction-induced mantle-wedge convection dominated the dynamics of East China, the minor upwelling mantle convection cells and following deviatoric tensional stresses could initiate and develop beneath the lithospheric base of these weak zones (e.g., Ziegler and Cloetingh, 2004; Yang et al., 2018a, 2018b). Extensional strain would preferentially localize on the pre-existing lithospheric weak zones within and around East China, resulting in crustal rifting and the development of sedimentary basins, such as the Lower Yangtze and Bohai Bay basins. The pre-existing crustal-scale mechanically weak zones not only control the occurrence of the minor upwelling mantle convection cell, but also contribute to the localization of extensional sedimentary basins (e.g., Ziegler and Cloetingh, 2004; Yang et al., 2018a, 2018b). In contrast, when subduction-induced plate boundary

compressional forces sufficiently prevailed across continental interior, the tectonic framework readily transformed from extension to contraction, which could be further accommodated by a regional lithospheric-scale strike-slip fault zone within the deforming zones, especially the TLFZ.

6.3. Late Cretaceous-Early Cenozoic Izanagi plate subduction and initial big wedge mantle formation

Subduction of the Izanagi-plate beneath East Asia probably initiated in the Early Jurassic (e.g., Wang et al., 2017; Liu et al., 2017a) and the subducting slab shallowed to flat-slab subduction in the middle-late Jurassic, possibly due to subduction of a positively buoyant oceanic plateau (e.g., Liu et al., 2010; Liu et al., 2019; Wu et al., 2019; Liu et al., 2021a). or a composite Yanshanian slab (Liu et al., 2021b). The flattened slab probably reached to the NSGL, where it steepened again (e.g., Liu et al., 2021a). We do not attempt to further discuss or interpret the origin of early, relatively flat subduction, and note that a steep-slab subduction model has also been proposed (Kusky et al., 2014; Li and Wang, 2018). However, the interaction with this early phase of subduction, slab rollback, and the overlying continental lithosphere of the Sino-Korea and Lower Yangtze blocks caused cratonic thinning and weakening (Li et al., 2015; Liu et al., 2017a; Wu et al., 2019; Liu et al., 2019; Liu et al., 2021a), which resulted in extensive Late Jurassic-Early Cretaceous magmatism, pervasive intraplate deformation, and facilitated the generation of Bohai Bay-Lower Yangtze basin province. The exact spatial-temporal configuration of this earliest phase of subduction is impossible to reconstruct as the Izanagi slab has sunk into the lower mantle, but the age, position, and geochemistry of magmatic rocks can provide important clues on this subduction history, which we discuss next.

Mesozoic magmatic trends across the Sino-Korea and Lower Yangtze blocks show a Jurassic westward sweep (200-150 Ma) of magmatism followed by a Cretaceous eastward sweep (150-100 Ma) (e.g., Zheng and Dai, 2018; Tang et al., 2018; Li et al., 2019; Wu et al., 2019; Liu et al., 2019). This pattern tracks the Mesozoic shallowing and steepening, respectively, of the Izanagi slab and eastward trench retreat (i.e., slab rollback), which has been interpreted to have caused removal and regeneration of the lithospheric mantle until Early Cretaceous (~100 Ma) (Liu et al., 2019). Evidenced by the occurrence of 147 Ma-aged mantle-derived basalts (Dong et al., 2019), the change in slab dip and initiation of rollback (or slab sinking) probably occurred between 145 and 150 Ma, causing asthenosphere upwelling. Subsequent mantle convective flow caused the cratonic lithospheric mantle to be eroded, marked by the formation of arc-like basalts, and thinned and then destructed to the peak time at 130-120 Ma (Liu et al., 2019; Wu et al., 2019). With the termination of lithospheric thinning and destruction, the removed lithospheric mantle was replaced by a juvenile oceanic-type mantle at 110 Ma (Liu et al., 2019), following with contemporaneous intraplate extensional deformation including rift basins, giant normal faults, metamorphic core complexes and magmatic domes (Lin et al., 2013; Lin and Wei, 2020; Li et al., 2014), while mantle-derived basalts transited to be OIB-like from the arc-like, with ca. 125 Ma indicating the cessation of lithospheric replacement (Liu et al., 2019).

During the Late Cretaceous-Cenozoic, voluminous alkali basalts were distributed across the Sino-Korea block, defining two age groups: 90-40 Ma and 25-0 Ma (Liu et al., 2019). The former is mainly marked by a time-increasing reverse correlation between $^{87}Sr/^{86}Sr$ and Eu/Eu*. Comparatively, the latter presents low Eu/Eu*, and more depleted $^{87}Sr/^{86}Sr$, and more importantly, is mixed with abundant light Mg-enriched recycled carbonate melts derived from the Pacific plate subduction (Li and Wang, 2018; Liu et al., 2019). These two discrete phases of basalt volcanism correlate with regional tectonic events across the Bohai Bay-Lower Yangtze region: the transition of TLFZ from extensional to dextral strike-slip at ca. 40 Ma (e.g., Huang et al., 2015, 2018) and of sedimentary basins from syn-rifting to post rifting at ca. 25 Ma (e.g., Ren et al., 2002) (Fig. 2), respectively, likely implying that all these Cenozoic geological observations are dominated by the Izanagi-Pacific oceanic plate subduction.

Modern high-resolution geophysical sections observe a big-mantle wedge related to the Cenozoic Pacific plate subduction along East Asia (Huang and Zhao, 2006; Liu et al., 2017b). Based on the known western Pacific subduction history, we argue that this mantle wedge was probably established during the Cretaceous, as subduction of the Izanagi oceanic plate transitioned from flat-slab subduction to normal subduction. Mantle convection within a big-mantle wedge driven by the Izanagi slab subduction would have modulated Late Cretaceous-Early Cenozoic intracontinental extensional deformation across East China (e.g., Richards and Engebretson, 1992; Zhu et al., 2019; Yang et al., 2018a,b; Zhong and Gurnis, 1995; Hager and O'Connell, 1981). Although the mantle wedge was likely established in the Cretaceous, the Izanagi slab subduction progressively involved younger oceanic slab at the trench as the Izanagi-Pacific mid-ocean ridge approached the subduction zone. Subduction of younger oceanic slab leads to a relatively stable trench (i.e., limited retreat) and relatively weak convection in the mantle wedge (e.g., Goes et al., 2017; Yang et al., 2018a, 2018b). Therefore, we here argue that the mantle wedge above the subducting Izanagi plate was less significant in driving upper plate extension than the wedge above the Pacific slab in the Cenozoic, as discussed in the next section.

6.4. Cenozoic Pacific subduction and subduction-induced mantle convection

Continued subduction of the Izanagi plate led to Early Eocene subduction and complete consumption of the Izanagi-Pacific mid-oceanic ridge (e.g., Whittaker et al., 2007; Wu and Wu, 2019). Hence, most of the Cenozoic subduction history along the eastern margin of the Asian continent involved subduction of the Pacific oceanic slab (Fig. 14), which became progressively younger at the subduction trench during the middle-late Cenozoic. It has long been known that plate-boundary conditions can affect intra-plate regions >3,000 km away from these plate boundaries (e.g., Clark et al., 2008; Dal Zilio et al., 2018; Schellart and Lister, 2005a, 2005b; Faccenna, 2010; Yang et al., 2018a), and the Cenozoic subduction of Pacific plate led to intra-plate deformation in the Bohai Bay-Lower Yangtze Cenozoic extensional basin province at least 2,000 km away from the Pacific plate subduction zone (estimated from reconstructions of the Japan Sea) (Fig. 1A). The coupling between East Asia Cenozoic intracontinental deformation and Pacific subduction has been explored in several classic works (e.g., Ren et al., 2002; Yin, 2010; Liu et al., 2017a; Ma et al., 2019; Liu et al., 2021a; Liu et al., 2021d). In particular, numerical modelling experiments demonstrate the importance of coupled plate subduction-mantle convection on the initiation and extent of back-arc extension (e.g., Hall, 2002, 2012; Leng and Gurnis, 2011; Nakakuki and Mura, 2013; Liu et al., 2017a, 2017b; Yang et al., 2018a, 2018b), satisfactorily describing the Cenozoic subduction of Pacific slab (Seton et al., 2015; Honda, 2016; Liu et al., 2017b; Wu and Wu, 2019). Subduction of young oceanic plates (<20 Ma) at the trench leads to a weaker driving force for mantle convection that results in no trench retreat and strong compression in the back-arc region (Yang et al., 2018a, 2018b). Due to the subduction of young (<20 Ma) Pacific oceanic slab, strong compression is expected across Bohai Bay-Lower Yangtze region during the Eocene (ca. 56-40), but the extensional regime would have been subjected to tensile stresses generated by Pacific subduction-related mantle convection and the sinking Izanagi plate (Figs. 14A and 15B). After the Eocene consumption of Izanagi-Pacific mid-ocean ridge, the newly subducting Pacific plate was relatively young, which drove compression in the upper plate and a relatively weak mantle convection zone (Figs. 15C and 15D). Owing to the transition of Pacific subduction direction from NNW to W (Fig. 2) (Müller et al., 2016), westward subduction-related compression may have exceeded mantle convection-related tension to trigger the initiation of major continent-scale fault systems (e.g., Sakhalin fault; Jolivet et al.,

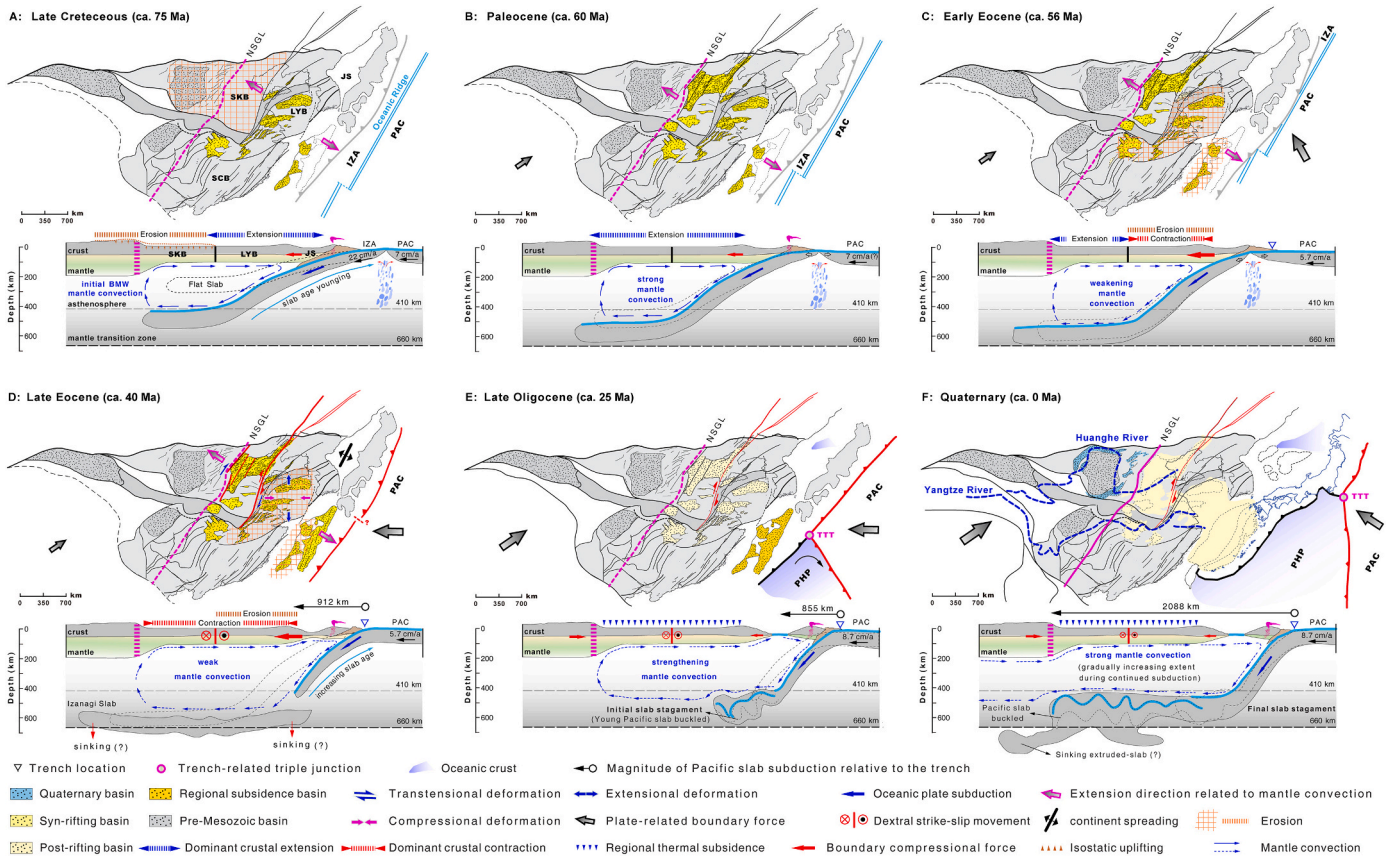

Fig. 15. Tectonic maps and integrated model for western Pacific subduction, mantle dynamics, and intraplate deformation in eastern China for various time slices: (A) Late Cretaceous (ca. 75 Ma), (B) Paleocene (ca. 60 Ma), (C) Early Eocene (ca. 56 Ma), (D) Late Eocene (ca. 40 Ma), (E) Late Oligocene (ca. 25Ma), and (F) Quaternary (ca. 0 Ma). The evolution of Cenozoic tectonics across east China is controlled by the subduction-related mantle convection of the big mantle wedge (BMW) and subduction-induced plate boundary forces. The size of these different indicators is proportional to the intensity of the corresponding geologic process. The magnitude of Pacific slab subduction is constrained by the slab velocity and the duration of its subduction from the trench. From Early Eocene (ca. 56 Ma) to Late Eocene (ca. 40 Ma), Late Eocene (ca. 40 Ma) to Late Oligocene (ca. 25 Ma), and Late Oligocene (ca. 25Ma) to Quaternary (ca. 0 Ma), the advanced distance is 912 km with the slab velocity of 5.7 cm/a (D), 855 km with that of 5.7 cm/a (E), and 2088 km with that of 8.7 cm/a (F), respectively. The slab velocity is derived from the newly-estimated velocity range of the Cenozoic Pacific plate (Fig. 2) (Jicha et al., 2018). BMW, Big mantle wedge; NSGL, North-South gravity lineament (Xu, 2007; Liu et al., 2021d); TTT, trench-trench-trench (TTT) triple junction system (Liu et al., 2017a; Ma et al., 2019; Liu et al., 2021d); PAC, Pacific plate; IZA, Izanagi plate; PHP, Philippine Sea plate; SKB, Sino-Korea block; LYB, Lower Yangtze block; SC, South China block; JS, Japan Sea.

1994), related initiation of Japan Sea spreading as a transtensional basin (e.g., Yin, 2010), and drive coupled TLFZ dextral faulting and Bohai Bay-Lower Yangtze deformation and erosion during the Late Eocene and Oligocene (ca. 45-20 Ma) (Figs. 14B and 15). The oceanic plate age rapidly increased at the trench, and starting in the Latest Oligocene-Early Miocene (ca. 25 Ma), subduction of older oceanic slab may have driven trench retreat (e.g., Nakakuki and Mura, 2013; Agrusta et al., 2017) with back-arc oceanic crust-floored opening, such as the Japan Sea (Fig. 15D) (Yang et al., 2018a, 2018b). Thus, these recent Eocene-to-present processes in eastern China may have been most strongly related to the age of the subducting slab.

Remarkably, all of the eastern China Cenozoic sedimentary basins transitioned from syn-rifting deposition to post-rifting thermal subsidence in the Late Oligocene (ca. 25 Ma) (e.g., Ren et al., 2002; Yin, 2010; Liu et al., 2017a), except for the East China Sea basin, which may have been strongly influenced by the Miocene westward subduction of the Philippine Sea plate during its Late Cenozoic basin evolution (Zhu et al., 2019; Wu et al., 2016; Liu et al., 2017a, 2021d) (Fig. 2 and Fig. 15). By assuming a constant subduction/convergence velocity, and ignoring variable slab morphology and subduction direction, we can use the best estimates of Late Cenozoic Pacific plate velocity (87 km/Ma) (Jicha et al., 2018) and the ~2,300 km length of the present-day seismically-imaged flatly-lying Pacific slab beneath the East Asia (e.g., Zhao and Ohtani, 2009; Wei et al., 2012; Chen et al., 2017) to estimate the duration that the Pacific slab advance in the MTZ from the Japan Trench to the slab's western edge beneath East China at ~26.4 million years. In other words, the flat Pacific slab has been in the MTZ for no more than 26 Ma, which is approximately consistent with the previous estimations: ~10-20 Ma (Liu et al., 2017b), or 24 Ma (e.g., Ma et al., 2019; Liu et al., 2021d). Considering the uncertainty and limitations of this calculation, it is interesting to note that the initial slab stagnation (ca. ~26 Ma) is almost coeval with the Late Oligocene syn-rifting-to-post-rifting transition (~25 Ma) across east China, as well as the time of oceanic crust formation in Japan Sea (e.g., Jolivet et al., 1994). We tentatively suggest that these key tectonic processes share a common geodynamic driver.

What triggered these major tectonic events in the Late Oligocene-Early Miocene (ca. 25 Ma)? Most regional studies of the plate-tectonic evolution of East Asia propose multiple drivers for this transition, including slab rollback-related trench retreat (e.g., Ren et al., 2002; Yin, 2010), slab tearing related to the clockwise rotation of Philippine Sea plate (Ma et al., 2019), and regional negative buoyancy-driven northwestward mantle flow (Liu et al., 2021d). It is notable that the subducted and stagnant slab has a lithospheric age of ~130 Ma near the Japan Trench that youngs to ~90 Ma near the slabs western tip (Liu et al., 2017b) (Fig. 1C). Constrained by the initial time of slab stagnation (ca. 25 Ma), the lithosphere age of the initial stagnated slab at the trench was approximately 65 Ma. Shallow subduction of relatively older slabs (>~60 Myr) may result in mantle wedge convection focused in the back-

arc region (~600 km away from the trench) that can generate sufficient driving force for back-arc sea spreading (e.g., Sdrolias and Müller, 2006; Yang et al., 2018a, 2018b), such as the Japan Sea initially floored by oceanic crust in the Late Oligocene-Miocene (e.g., Jolivet et al., 1994). As the slab became progressively older during Pacific plate subduction, the older oceanic slab favors subduction at a moderate angle (e.g., Salze et al., 2018; Yang et al., 2018a,b; Agrusta et al., 2017), triggering strong wedge mantle convection, trench retreat, and weaker plate-continent compression (Fig. 15). In addition, trench retreat and back-arc opening are all the indicators and tectonic responses of such plate subduction-mantle convection dynamics. Accordingly, here we propose that the age of the Pacific oceanic plate is one of the most important controls for these key tectonic processes mentioned above.

Whether the large horizontal Pacific slab lying in the MTZ is related to the Late Oligocene syn-rift-to-post-rift transition across East China is an open question (e.g., Liu et al., 2017a; Ma et al., 2019; Liu et al., 2021d). High-resolution seismic tomography reveal that the flat-lying Pacific slab is >150 km thick (with a maximum thickness of ~200 km) in the MTZ beneath the East China (e.g., Zhao and Ohtani, 2009; Wei et al., 2012; Chen et al., 2017; Liu et al., 2017b), which is much thicker than the thickness (~80-100 km) of the Pacific slab at the Japan Trench revealed by local tomography and receiver functions results (e.g., Kawakatsu et al., 2009; Liu and Zhao, 2016; Zhao et al., 2012). Owing to the age-dependence of oceanic slab thickness (Kawakatsu et al., 2009), the older Pacific slab at the trench should be thicker than the younger flat slab in the MTZ. However, the contradiction of stagnated slab thickness between theory and observation in the MTZ beneath the East China imply that the hotter, thinner, younger subducted oceanic slab may be compressively thickened and buckled in the MTZ (Goes et al., 2017; Ribe et al., 2007; Yang et al., 2018a, 2018b).

Additional support for this hypothesis comes from considerations of relative plate motion (Fig. 15). From the Eocene to the Quaternary (56-0 Ma), the Pacific slab at the trench cumulatively subducted at least 3,800 km relative to the trench (Fig. 15), but the seismically imaged length of this slab is only about 2,300 km (Fig. 1C), most likely indicating that the 1,500-km differential distance of slab advance should be probably consumed in the MTZ (Fig. 15E and 15F). Moreover, with the continuous subduction of rapidly-aging Pacfic slab at the trench, the young and thin Pacific slab should be gradually buckled when it penetrated into the MTZ, initiating slab stagnation (Fig. 15E). When the thickness and mechanical strength of the subducted old slab (> ~60Ma) could resist the buckling deformation after the Miocene, the accumulated Pacific slab could advance horizontally in the MTZ to East China continental interior (Fig. 15F). Simulated by the numerical modelling (Yang et al., 2018a, 2018b), the initiation and development of the slab stagnation could gradually increase the extent of subduction-driven mantle convection cell, which would exert a more distributed and weaker basal traction on the overlying continent, thus leading to the cessation of rifting and syn-rift sedimentation to initiate post-rifting subsidence across East China (Figs. 15E and 15F). After the Miocene, during the process of slab stagnation and associated slab rollback, renewed upwelling flow as part of a very large mantle convection cell initiated beneath the major lithospheric-scale weak zones, such as the ~Baikal Lake region above the Siberia-Amuria plate boundary, ~3,000-km to the WNW (Yang et al., 2018a, 2018b) (Fig. 15F). This shift focused extension away from East China, and implies that lateral rheological heterogeneity of the continental lithosphere may focus upwelling of subduction-induced mantle convection (Yang et al., 2018a, 2018b).

6.5. *Subduction-induced boundary conditions and plate-mantle coupling: Implication for East China Cenozoic tectonics*

Here we present an updated plate-mantle coupling model to describe the kinematics of Cenozoic tectonics across East China that reconstructs Izanagi-Pacific subduction and the structural-sedimentological evolution of the east China basin province since the Late Cretaceous. The model is constrained by recent geological observations and numerical modelling (e.g., Liu et al., 2017a; Yang et al., 2018a, 2018b; Jicha et al., 2018; Wu and Wu, 2019; Ma et al., 2019; Liu et al., 2021a, 2021d).

6.5.1. *Late Cretaceous-Early Cenozoic (75-56 Ma) regional extension during Izanagi plate subduction*

Following the cessation of Late Jurassic-Early Cretaceous lithospheric weakening and thinning, characterized by intracontinental extensive magmatism and extension (Wu et al., 2019; Liu et al., 2019; Liu et al., 2021b), the old Izanagi slab transitioned from flat-slab subduction to steep subduction (e.g., Liu et al., 2021a), forming an initial mantle wedge zone that drove strong mantle flow convection. The mantle drag force on the continental lithosphere drove extension across eastern China, possibly focusing deformation on pre-existing fabrics, and basins across the region received sedimentary deposits during the Late Cretaceous (ca. 75-65 Ma) (Liu et al., 2017a). The one exception is the Bohai Bay basin, west of the TLFZ, which mostly lacks Late-Cretaceous deposits due to presumed widespread uplift (Fig. 15A). Although denudation across the North China region is generally interpreted as an episode of flat-slab subduction of the Izanagi plate (Liu et al., 2020), this tectonic regime contradicts with the coeval sedimentary sequence within the Subei-South Yellow Sea basin. One explanation for these differences might be that the North China region experienced Mesozoic cratonic lithospheric delamination, and the asethenospheric upwelling may have heated the lithosphere to increase the residual lithospheric buoyancy, causing isostatic uplift (e.g., Liu et al., 2021a).

After ca. 65 Ma, the Izanagi slab increasingly transformed from flat to steep subduction, forming an initial mantle wedge with relatively strong convection (Fig. 15B). Mantle drag forces led to extensive intraplate crustal stretching across east China, producing a series of syn-rift sedimentary basins (Fig. 15B). Through time, this convection cell weakened as the slab age became younger and the mid-ocean ridge collided with the trench (Fig. 15C).

6.5.2. *Early-Middle Cenozoic (56-25 Ma) mid-ocean ridge collision and onset of Pacific subduction*

At ca. 56 Ma, the Izanagi-Pacific mid-ocean spreading ridge collided with the subduction zone, which is recorded by a regional sedimentary unconformity in the east China basin province, except for the Bohai Bays due to its location far away from the subduction zone (Fig. 15C). Subsequently, after the Izanagi plate and Izanagi-Pacific mid-oceanic ridge are completely consumed beneath the East Asia continent, continuous extension is attributed to the subduction of aging Pacific slab (Fig. 15D). As indicated by the Hawaiian-Emperor Chain bend (Torsvik et al., 2017) dated to 49.4 Ma (Jicha et al., 2018), the direction of north-western Pacific oceanic plate motion relative to the northeast Asia abruptly changes from NNW to NWW in the Eocene (ca. 50 Ma). A correlative shift in regional unconformities is observed in these sedimentary basins around the TLFZ, such as Bohai Bay, Lower Yangtze and Jianghan basins (Fig. 2). During the Early Eocene, the relatively young Pacific oceanic plate continued its counter-clockwise rotation and subducted westward, approximately perpendicular to the subduction zone (Fig. 2) (Müller et al., 2016), which resulted in an especially strong plate boundary force and relatively weak mantle convection that initiated TLFZ dextral movement and coeval coupled deformation of Lower Yangtze and Bohai Bay regions (Fig. 15D). While the Lower Yangtze region was dragged south-westward by the TLFZ, it underwent EW-oriented shortening and northward stretching, and the Bohai Bay region experienced transtensional and strike-slip deformation dominated by the TLFZ-related dextral strike-slip faults. In such a tectonic setting, the Lower Yangtze region to the east of the TLFZ was denuded, as well as the western portion of the East China Sea basin (Fig. 15D).

6.5.3. *Late Cenozoic (25-0 Ma) extensional deformation*

During the Miocene, the western Pacific oceanic plate continued to subduct westward (Liu et al., 2017a). The Pacific slab began to initially

stagnate in the MTZ at ca. 25 Ma with the younger slab buckling and thickening, which led to the establishment of a large mantle convection cell. The large extent of this convection cell led to relatively weak basal traction on the overlying continental crust, and therefore extension and syn-rift sedimentation ceased in East Asia (Fig. 15E). The age of the oceanic slab at the trench gradually became older (>~60 Ma), which drove the trench to retreat and was accompanied by strong back-arc spreading, exemplified by the Japan Sea opening (e.g., Jolivet et al., 1994; Yang et al., 2018a, 2018b). Furthermore, with continuous clockwise rotation, the Philippine Sea plate started obliquely converging with the Eurasian continent in the Late Oligocene (at ca. 25 Ma), and further moved northward to subduct beneath eastern Asia and generate a trench-trench-trench (TTT) triple junction (Ma et al., 2019; Liu et al., 2021d), intensively influencing the evolution of East China Sea basin evidenced by basin inversion (e.g., Su et al., 2014) and regional Miocene subsidence (e.g., Zhu et al., 2019) (Fig. 2 and Fig. 15E). This likely facilitated slab stagnation formation and Japan Sea opening (e.g., Liu et al., 2021d) (Figs. 15D-15E).

Although the wedge mantle convection was strengthened by subduction of the progressively older Pacific slab, the subduction-induced wedge mantle zone gradually increased its convecting extent during this process, which could have driven extension in the Baikal Rift Zone, ~3000 km away from the Japan trench (e.g., Yang et al., 2018a, 2018b). In such setting, the vigor of mantle convection beneath eastern China may have been relatively weak, and therefore, intra-plate deformation is subdued (Fig. 15F). Since the Miocene, the eastern China basin province is dominated by regional subsidence, covered by Neogene-Quaternary sediments (e.g., Ren et al., 2002). They could have been largely filled by the influxes of sediments from the Yangtze and Huanghe Rivers (Fig. 15F), dated at Late Oligocene (ca. 24 Ma) (e.g., Zheng et al., 2013) or Late Miocene (ca. ~12 Ma) (e.g., Fu et al., 2021). Since the Neogene, much of the Himalayan-Tibetan orogeny experienced widespread intracontinental extension (Tapponnier et al., 2001; Yin et al., 1999; Yin, 2010; Bian et al., 2020), especially the Ordos rift system composed of the Yinchuan, Hetao, and Shanxi grabens (e.g., Zhang et al., 2003; Yin, 2010). This time period marks the onset of the eastward extrusion tectonics, which influence the east-west, inland extension within Asia. As illustrated with seismic tomography (Huang and Zhao, 2006) and numerical modelling (Liu and Nummedal, 2004), the Taihang-Wuning-Xuefeng mountains constitute the easternmost boundary of the far-field effect of the India-Eurasia collision. Facilitated and enhanced by the collision-induced stress state, the TLFZ continued to experience dextral strike-slip motion until present (Fig. 15F).

The abrupt change in lithospheric thickness and topography across the NSGL marks the western extent of the continental-scale Cenozoic basin province discussed in this work (e.g., Liu et al., 2021a). The transition is located 2,000 km and 1,000 km away from the Indian and Pacific plate boundaries, respectively (Fig. 15F). This transitional zone is impacted by both the Pacific tectonic domain to the east and the Neo-Tethyan tectonic domain to the west-southwest (Xu, 2007; Zhao and Ohtani, 2009; Liu et al., 2021a). Geologically, the NSGL is a crucial indicator of the evolution of the lithosphere and topography within East China since the Cretaceous, and also an important tectonic record of Mesozoic-Cenozoic Izanagi-Pacific plate subduction (Fig. 15) (Liu et al., 2021a). It represents the eastern and western boundaries of plate margin-related tectonics of the India-Asia collision and Pacific-Asia convergence, respectively, of which the east region may be dominated by the Pacific tectonic domain.

6.6. Limitations and future work

This synthesis was based primarily on the sedimentary basin history across the Lower Yangtze region and eastern China, but further research on the intra-plate rift-related volcanism will provide important new insights to explore coupling between plate-boundary conditions and mantle convection along the western Pacific. Moreover, the coupling between Cenozoic oceanic slab subduction and mantle convection is currently quantified based on 2-D numerical models (e.g., Yang et al., 2018a, 2018b), but additional 3-D models with possibly more realistic geometry and rheology are needed in the future to advance our knowledge of the dynamics of the plate subduction-mantle convection, providing more realistic constraint on the intraplate deformation process and basin evolution. Natural settings are intrinsically 3D, and lateral upper and lower plates heterogeneities can affect the slab behaviour (such as dip angle and velocity) (e.g., Billen, 2008; Faccenda and Capitanio, 2012; Liu et al., 2021d). Especially, the role of slab age on the mantle-convection dynamics should be further verified in 3-D modelling framework. Out-of-plane fault motion, migrating triple junctions, and oblique subduction all suggest complex 3D kinematics. In future work, the complexity of 3D geological model should be further considered and addressed.

Moreover, there is a complex issue of simultaneous contractional and extensional intraplate deformation, such as Late Cretaceous East Asian basin inversion/compression (Liu et al., 2017a) and fast uplift/exhumation along the Great Xing'an-Taihang-Xuefeng Mountains (Liu et al., 2021a) at the same time as coeval with the Lower Yangtze extension/subsidence (this study). Although the model presented in this study invokes the mantle convection cell to explain these differences, alternative scenarios could be envisioned. For example, in the western U.S during Laramide flat slab subduction, there is a similar occurrence where extensive inland compression occurred (Saleeby, 2003; Liu et al., 2010; Axen et al., 2018) at the same time as local extension along the California margin (e.g., Jacobson et al., 2007; Liu et al., 2010; Chapman et al., 2010), which has been related to local collapse due to gravitational instabilities. Although the scale of these features are different, future work comparing and contrasting these orogens across the Pacific realm may provide important intriguing insights.

7. Conclusions

The Late Cretaceous-Cenozoic sedimentary basins in east China evolved as a series of structural and geochronological archives of the continental margin interactions between the Izangi-Pacific subduction system and overlying eastern Asian continent during the Late Mesozoic and Cenozoic, providing solid constraints for the intracontinental deformational response to plate boundary dynamics. In terms of integrated geological and geophysical synthesis of these archives, we present an updated geological model for intracontinental deformation driven by plate-boundary forces and mantle-wedge dynamics. The formation of the mantle wedge during the consumption of oceanic slab can be divided into two stages: 1) initial mantle wedge convection before the Izanagi-Pacific ridge subduction and 2) mature mantle wedge convection after the ridge subduction. The former is driven by the switch of the Izanagi slab geometry from flat to steep, whereas the latter is directly controlled by the Pacific slab age at the trench. West-dipping Izanagi-plate subduction in the Late Cretaceous-Paleocene was not flat but relatively steep, leading to upper plate strong extension of eastern China coupled with strong mantle convection in the initial mantle wedge. Eocene collision of the mid-ocean ridge separating the Izanagi-Pacific plates led to a gap in magmatism and regional uplift across eastern China. Subsequent westward subduction of the rapidly-aging Pacific slab triggered strong convection with an increasing extent (relatively weak convection at the continent scale), correspondingly generating weak intracontinental extension. During Cenozoic subduction, the age of Izanagi-Pacific oceanic slab serves as a potential proxy of kinematic-dynamic interactions between convergent continental-oceanic plate and convecting mantle, which is consistent with the evolution of the overriding intracontinental extension and continent-marginal back-arc basin. Furthermore, the right-slip TLFZ was dynamically driven by the westward movement of Pacific plate, which remarkably partitioned contractional strain between Bohai Bay and Lower Yangtze basins.

Declaration of Competing Interest

We confirm that there are no known conflicts of interest associated with this publication and there has been no significant financial support for this work that could have influenced its outcome.

Acknowledgements

Xi Xu greatly appreciates Prof. Zuyi Zhou of Tongji University, his doctoral supervisor, for his ongoing guidance, encouragement and support on this study, and Prof. Fengli Yang of Tongji University, his master supervisor, for her important enlightenment on tectonics research in the Lower Yangtze region. We thank Dr. Ting Yang of South University of Science and Technology of China (SUSTC) for sincere discussion on the plate-mantle system. This work is further financially supported by the grants from the National Natural Science Foundation of China (No. 41902202), National Science Foundation (EAR 1914501), Chinese Postdoctoral Science Foundation (No. 2019M652062), Key Laboratory of Airborne Geophysics and Remote Sensing Geology Ministry of Natural Resources (No. 2020YFL13), State Key Scientific Research Program of China (No. 2011ZX0523-003), and Geological Survey Project of China (No. DD20211396). We thank Dr. Manuele Faccenda and one anonymous reviewer for their sincere and constructive comments. We also thank Chief Editor Douwe van Hinsbergen and Guest Editor Lijun Liu for their editorial efforts and directional suggestions. Data processing and plot illustrating were supported by the GMT package (Wessel and Smith, 1998).

References

Agrusta, R., Goes, S., Van Hunen, J., 2017. Subducting-slab transition-zone interaction: Stagnation, penetration and mode switches. Earth Planet. Sci. Lett. 464, 10–23.
AHBGMR Anhui Bureau of Geology and Mineral Resources, 1987. Regional Geology of Anhui Province. Geological Publishing House, Beijing, pp. 1–721.
Allen, M.B., Macdonald, D., Xun, Z., Vincent, S.J., Brouet-Menzies, C., 1997. Early Cenozoic two-phase extension and late Cenozoic thermal subsidence and inversion of the Bohai Basin, northern China. Mar. Pet. Geol. 14 (7-8), 951–972.
Allen, M.B., Macdonald, D.I., Xun, Z., Vincent, S.J., Brouet-Menzies, C., 1998. Transtensional deformation in the evolution of the Bohai Basin, northern China. Geol. Soc. Lond., Spec. Publ. 135 (1), 215–229.
An, K., Lin, X.B., Wu, L., Yang, R., Chen, H.L., Cheng, X.G., Xia, Q.K., Zhang, F.Q., Ding, W.W., Gao, S.B., 2020. An immediate response to the Indian-Eurasian collision along the northeastern Tibetan Plateau: evidence from apatite fission track analysis in the Kuantan Shan-Hei Shan. Tectonophysics 774, 228278.
Axen, G.J., van Wijk, J.W., Currie, C.A., 2018. Basal continental mantle lithosphere displaced by flat-slab subduction. Nat. Geosci. 11 (12), 961–964.
Becker, J.J., Sandwell, D.T., Smith, W.H.F., Brad, J., Binder, B., Depner, J.L., Fabre, D., Factor, J., Ingalls, S., Kim, S.H., 2009. Global bathymetry and elevation data at 30 arc seconds resolution: SRTM30_PLUS. Mar. Geod. 32 (4), 355–371.
Bellahsen, N., Faccenna, C., Funiciello, F., 2005. Dynamics of subduction and plate motion in laboratory experiments: insights into the "plate tectonics" behavior of the Earth. J. Geophys. Res. Solid Earth 110 (B1).
Bian, S., Gong, J.F., Zuza, A.Z., Yang, R., Tian, Y.T., Jianqing, Ji, Chen, H.L., Xu, Q.Q., Chen, L., Lin, X.B., 2020. Late Pliocene onset of the Cona rift, eastern Himalaya, confirms eastward propagation of extension in Himalayan-Tibetan orogen. Earth Planet. Sci. Lett. 544, 116383.
Billen, M.I., 2008. Modeling the dynamics of subducting slabs. Annu. Rev. Earth Planet. Sci. 36, 325–356.
Cao, Z.X., 2008. Calculation of extension and subsidence of the Cenozoic pull-apart and rift basins along the Yingkou-Weifang fault zone. Chin. J. Geol. 43 (1), 65–81.
Capitanio, F.A., Morra, G., Goes, S., 2007. Dynamic models of downgoing plate-buoyancy driven subduction: Subduction motions and energy dissipation. Earth Planet. Sci. Lett. 262 (1-2), 284–297.
Carlson, R.L., Hilde, T.W.C., Uyeda, S., 1983. The driving mechanism of plate tectonics: relation to age of the lithosphere at trenches. Geophys. Res. Lett. 10 (4), 297–300.
Cawood, P.A., Kroner, A., Collins, W.J., Kusky, T.M., Mooney, W., Wndley, B., 2009. Accretionary orogens through Earth history. Geol. Soc. Lond., Spec. Publ. 318 (1), 1–36.
Celaya, M., McCabe, R., 1987. Kinematic model for the opening of the Sea of Japan and the bending of the Japanese islands. Geology 15 (1), 53–57.
Chang, K., Park, S., 2001. Paleozoic Yellow Sea Transform Fault: its role in the tectonic history of Korea and adjacent regions. Gondwana Res. 4 (4), 588–589.
Chang, K., Zhao, X., 2012. North and South China suturing in the east end: What happened in Korean Peninsula? Gondwana Res. 22 (2), 493–506.
Chapman, A.D., Kidder, S., Saleeby, J.B., Ducea, M.N., 2010. Role of extrusion of the Rand and Sierra de Salinas schists in Late Cretaceous extension and rotation of the southern Sierra Nevada and vicinity. Tectonics 29 (5).
Charles, N., et al., 2013. Timing, duration and role of magmatism in wide rift systems: Insights from the Jiaodong Peninsula (China, East Asia). Gondwana Res. 24 (1), 412–428.
Charvet, J., Shu, L., Shi, Y., Guo, L., Faure, M., 1996. The building of south China: collision of Yangzi and Cathaysia blocks, problems and tentative answers. J. SE Asian Earth Sci. 13 (3-5), 223–235.
Chen, W.P., Nábelek, J., 1988. Seismogenic strike-slip faulting and the development of the North China Basin. Tectonics 7 (5), 975–989.
Chen, L., Zheng, T., Xu, W., 2006. A thinned lithospheric image of the Tanlu Fault Zone, eastern China: constructed from wave equation based receiver function migration. J. Geophys. Res. Solid Earth 111 (B9).
Chen, C., et al., 2017. Mantle transition zone, stagnant slab and intraplate volcanism in Northeast Asia. Geophys. J. Int. 209 (1), 68–85.
Cheng, F., Garzione, C.N., Jolivet, M., Guo, Z., Zhang, D., Zhang, C., Zhang, Q., 2019. Initial deformation of the northern Tibetan plateau: insights from deposition of the Lulehe Formation in the Qaidam Basin. Tectonics 38 (2), 741–766.
Clark, S.R., Stegman, D., Müller, R.D., 2008. Episodicity in back-arc tectonic regimes. Phys. Earth Planet. Inter. 171 (1-4), 265–279.
Conrad, C.P., Lithgow-Bertelloni, C., 2002. How mantle slabs drive plate tectonics. Science 298 (5591), 207–209.
Dal Zilio, L., Faccenda, M., Capitanio, F., 2018. The role of deep subduction in supercontinent breakup. Tectonophysics 746, 312–324.
DeCelles, P.G., 2004. Late Jurassic to Eocene evolution of the Cordilleran thrust belt and foreland basin system, western USA. Am. J. Sci. 304 (2), 105–168.
DeCelles, P.G., Kapp, P., Gehrels, G.E., Ding, L., 2014. Paleocene-Eocene foreland basin evolution in the Himalaya of southern Tibet and Nepal: Implications for the age of initial India-Asia collision. Tectonics 33 (5), 824–849.
Dickinson, W.R., Snyder, W.S., Matthews, V., 1978. Plate tectonics of the Laramide orogeny. Geological Society of America Memoir 151, Matthews. Vol. 3, 355–366.
Dilek, Y., Altunkaynak, F., 2009. Geochemical and temporal evolution of Cenozoic magmatism in western Turkey: mantle response to collision, slab break-off, and lithospheric tearing in an orogenic belt. Geol. Soc. Lond., Spec. Publ. 311 (1), 213–233.
Ding, D.G., Wang, D.Y., Liu, Y.L., 2009. Transformation and deformation of the Paleozoic basins in lower Yangtze areas. Earth Sci. Front. 16 (4), 61–73.
Dong, J., et al., 2019. Onset of the North-South Gravity Lineament, NE China: constraints of late Jurassic bimodal volcanic rocks. Lithos 334, 58–68.
Dong, Y., Liu, X., Neubauer, F., Zhang, G., Tao, N., Zhang, Y., ...Li, W., 2013. Timing of Paleozoic amalgamation between the North China and South China Blocks: evidence from detrital zircon U–Pb ages. Tectonophysics 586, 173–191.
Faccenda, M., Capitanio, F.A., 2012. Development of mantle seismic anisotropy during subduction-induced 3-D flow. Geophys. Res. Lett. 39, L11305.
Faccenna, C., Heuret, A., Funiciello, F., Lallemand, S., Becker, T., 2007. Predicting trench and plate motion from the dynamics of a strong slab. Earth Planet. Sci. Lett. 257 (1-2), 29–36.
Faccenna, C., et al., 2010. Subduction-triggered magmatic pulses: A new class of plumes? Earth Planet. Sci. Lett. 299 (1-2), 54–68.
Faure, M., et al., 2003. Exhumation tectonics of the ultrahigh-pressure metamorphic rocks in the Qinling orogen in east China: New petrological-structural-radiometric insights from the Shandong Peninsula. Tectonics 22 (3).
Finzel, E.S., Flesch, L.M., Ridgway, K.D., Holt, W.E., Ghosh, A., 2015. Surface motions and intraplate continental deformation in Alaska driven by mantle flow. Geophys. Res. Lett. 42 (11), 4350–4358.
Fu, X., Zhu, W., Geng, J., Yang, S., Zhong, K., Huang, X., Xu, X., 2021. The present-day Yangtze River was established in the late Miocene: Evidence from detrital zircon ages. J. Asian Earth Sci. 205, 104600.
Gao, S., Xu, X., Zhou, Z., 2015. Structural deformation and genesis of the northern sub-basin in South Yellow Sea since Late Cretaceous. Oil Gas Geol. 36 (6), 924–933.
Garel, F., et al., 2014. Interaction of subducted slabs with the mantle transition-zone: A regime diagram from 2-D thermo-mechanical models with a mobile trench and an overriding plate. Geochem. Geophys. Geosyst. 15 (5), 1739–1765.
Gilder, S.A., et al., 1999. Tectonic evolution of the Tancheng-Lujiang (Tan-Lu) fault via middle Triassic to Early Cenozoic paleomagnetic data. J. Geophys. Res. Solid Earth 104 (B7), 15365–15390.
Goes, S., Capitanio, F.A., Morra, G., Seton, M., Glardini, D., 2011. Signatures of downgoing plate-buoyancy driven subduction in Cenozoic plate motions. Phys. Earth Planet. Inter. 184 (1–2), 1–13.
Goes, S., Agrusta, R., van Hunen, J., Garel, F., 2017. Subduction-transition zone interaction: A review. Geosphere 13 (3), 644–664.
Gong, Z.S., Zhu, W.L., Chen, P.P.H., 2010. Revitalization of a mature oil-bearing basin by a paradigm shift in the exploration concept: a case history of Bohai Bay, Offshore China. Mar. Pet. Geol. 27, 1–17.
Grimmer, J.C., et al., 2002. Cretaceous-Cenozoic history of the southern Tan-Lu fault zone: apatite fission-track and structural constraints from the Dabie Shan (eastern China). Tectonophysics 359 (3-4), 225–253.
Hacker, B.R., Wallis, S.R., Ratschbacher, L., Grove, M., Gehrels, G., 2006a. High-temperature geochronology constraints on the tectonic history and architecture of the ultrahigh-pressure Dabie-Sulu Orogen. Tectonics 25 (5).
Hacker, B.R., Wallis, S.R., Ratschbacher, L., Grove, M., Gehrels, G., 2006b. High-temperature geochronology constraints on the tectonic history and architecture of the ultrahigh-pressure Dabie-Sulu Orogen. Tectonics 25 (5).
Hall, R., 2002. Cenozoic geological and plate tectonic evolution of SE Asia and the SW Pacific: computer-based reconstructions, model and animations. J. Asian Earth Sci. 20 (4), 353–431.
Hall, R., 2012. Late Jurassic–Cenozoic reconstructions of the Indonesian region and the Indian Ocean. Tectonophysics 570, 1–41.

Han, W.G., Ji, J.Q., Wang, J.D., Yu, J.G., Zhang, X.Y., Yu, S.L., 2005. Paleocene-Early Eocene sinistral strike-slipping of the Tan-Lu fault zone: evidence fromreflection seismic exploration(in Chinese). Prog. Nat. Sci. 15 (11), 1383–1388.
Hao, T., et al., 2003. Deep structure characteristics and geological evolution in Yellow Sea and adjacent region. Chin. J. Geophys. 46 (6), 1148–1156.
Hao, T., et al., 2007. East Marginal Fault of the Yellow Sea: a part of the conjunction zone between Sino-Korea and Yangtze Blocks? Geological Society, London. Special Publications 280 (1), 281–291.
Hager, B.H., O'Connell, R.J., 1981. A simple global model of plate dynamics and mantle convection. J. Geophys. Res. Solid Earth 86 (B6), 4843-4867.
HBBGMR Hubei Bureau of Geology and Mineral Resources, 1990. Regional Geology of Hubei Province. Geological Publishing House, Beijing, pp. 1–705.
Holt, A.F., Becker, T.W., Buffett, B.A., 2015. Trench migration and overriding plate stress in dynamic subduction models. Geophys. J. Int. 201 (1), 172–192.
Honda, S., 2016. Slab stagnation and detachment under northeast China. Tectonophysics 671, 127–138.
Hou, G., Hari, K.R., 2014. Mesozoic-Cenozoic extension of the Bohai Sea: contribution to the destruction of North China Craton. Front. Earth Sci. 8 (2), 202–215.
Hsiao, L., Graham, S.A., Tilander, N., 2004. Seismic reflection imaging of a major strike-slip fault zone in a rift system: Paleogene structure and evolution of the Tan-Lu fault system, Liaodong Bay, Bohai, offshore China. AAPG Bull. 88 (1), 71–97.
Hsiao, L.Y., Graham, S.A., Tilander, N., 2010. Stratigraphy and sedimentation in a rift basin modified by synchronous strike-slip deformation: Southern Xialiao basin, Bohai, offshore China. Basin Res. 22 (1), 61–78.
Hu, X., Garzanti, E., Moore, T., Raffi, I., 2015. Direct stratigraphic dating of India-Asia collision onset at the Selandian (middle Paleocene, 59.1 Ma). Geology 43 (10), 859–862.
Hu, X., et al., 2016. The timing of India-Asia collision onset–Facts, theories, controversies. Earth Sci. Rev. 160, 264–299.
Huang, L., Liu, C.Y., 2014. Evolutionary characteristics of the sags to the east of Tan–Lu Fault Zone, Bohai Bay Basin (China): Implications for hydrocarbon exploration and regional tectonic evolution. J. Asian Earth Sci. 79, 275–287.
Huang, J., Zhao, D., 2006. High-resolution mantle tomography of China and surrounding regions. J. Geophys. Res. Solid Earth 111 (B9).
Huang, L., Liu, C., Zhou, X., Wang, Y., 2012. The important turning points during evolution of Cenozoic basin offshore the Bohai Sea: Evidence and regional dynamics analysis. Sci. China Earth Sci. 55 (3), 476–487.
Huang, L., Liu, C., Kusky, T.M., 2015. Cenozoic evolution of the Tan-Lu Fault Zone (East China): Constraints from seismic data. Gondwana Res. 28 (3), 1079–1095.
Huang, L., Liu, C.Y., Xu, C.G., Wu, K., Wang, G.Y., Jia, N., 2018. New insights into the distribution and evolution of the Cenozoic Tan-Lu Fault Zone in the Liaohe sub-basin of the Bohai Bay Basin, eastern China. Tectonophysics 722, 373–382.
Ingersoll, R.V., 2019. Subduction-related sedimentary basins of the US Cordillera. The sedimentary basins of the United States and Canada. Elsevier, pp. 477-510.
Jacobson, C.E., Grove, M., Vucic, A., Pedrick, J.N., Ebert, K.A., Cloos, M., 2007. Exhumation of the Orocopia Schist and associated rocks of southeastern California: Relative roles of erosion, synsubduction tectonic denudation, and middle Cenozoic extension. Special Papers-Geological Society of America 419, 1.
Jiang, Q., 2013. Fault genesis analysis and numerical modeling for the southern fault step zone in the Gaoyou Sag. Heifei University of Technology, Heifei.
Jiang, R., Cao, K., Zeng, J., Liu, K., Li, C., Wang, A., Zhao, L., 2019. Late Cenozoic tectonic evolution of the southern segment of the Tan-Lu fault zone, Eastern China. J. Asian Earth Sci. 182, 103932.
Jicha, B.R., Garcia, M.O., Wessel, P., 2018. Mid-Cenozoic Pacific plate motion change: Implications for the northwest Hawaiian Ridge and circum-Pacific. Geology 46 (11), 939–942.
Jolivet, L., Huchon, P., Rangin, C., 1989. Tectonic setting of Western Pacific marginal basins. Tectonophysics 160 (1-4), 23–47.
Jolivet, L., Davy, P., Cobbold, P., 1990. Right-lateral shear along the northwest Pacific margin and the India-Eurasia collision. Tectonics 9 (6), 1409–1419.
Jolivet, L., Tamaki, K., Fournier, M., 1994. Japan Sea, opening history and mechanism: A synthesis. J. Geophys. Res. Solid Earth 99 (B11), 22237–22259.
JSBGMR Jiangsu Bureau of Geology and Mineral Resources, 1987. Regional Geology of Jiangsu Province and Shanghai City. Geological Publishing House, Beijing, pp. 1–857.
JXBGMR Jiangxi Bureau of Geology and Mineral Resources, 1984. Regional Geology of Jiangxi Province. Geological Publishing House, Beijing, pp. 1–921.
Kapp, P., DeCelles, P.G., 2019. Mesozoic–Cenozoic geological evolution of the Himalayan-Tibetan orogen and working tectonic hypotheses. Am. J. Sci. 319 (3), 159–254.
Kawakatsu, H., Kumar, P., Takei, Y., Shinohara, M., Kanazawa, T., Araki, E., Suyehiro, K., 2009. Seismic evidence for sharp lithosphere-asthenosphere boundaries of oceanic plates. Science 324 (5926), 499–502.
Kimura, G., Tamaki, K., 1986. Collision, rotation, and back-arc spreading in the region of the Okhotsk and Japan Seas. Tectonics 5 (3), 389–401.
King, S.D., Frost, D.J., Rubie, D.C., 2015. Why cold slabs stagnate in the transition zone. Geology 43 (3), 231–234.
Kusky, T.M., et al., 2014. Flat slab subduction, trench suction, and craton destruction: Comparison of the North China, Wyoming, and Brazilian cratons. Tectonophysics 630, 208–221.
Lallemand, S., Jolivet, L., 1986. Japan Sea: a pull-apart basin? Earth Planet. Sci. Lett. 76 (3-4), 375–389.
Lallemand, S., Heuret, A., Boutelier, D., 2005. On the relationships between slab dip, back-arc stress, upper plate absolute motion, and crustal nature in subduction zones. Geochem. Geophys. Geosyst. 6 (9).
Lee, T., Lawver, L.A., 1995. Cenozoic plate reconstruction of Southeast Asia. Tectonophysics 251 (1-4), 85–138.
Leng, W., Gurnis, M., 2011. Dynamics of subduction initiation with different evolutionary pathways. Geochem. Geophys. Geosyst. 12 (12).
Li, S., Kusky, T.M., Wang, L., Zhang, G., Lai, S., Liu, X., Zhao, G., 2007. Collision leading to multiple-stage large-scale extrusion in the Qinling orogen: insights from the Mianlue suture. Gondwana Research 12 (1–2), 121–143.
Li, Z., Li, X., 2007. Formation of the 1300-km-wide intracontinental orogen and postorogenic magmatic province in Mesozoic South China: a flat-slab subduction model. Geology 35 (2), 179–182.
Li, S., Wang, Y., 2018. Formation time of the big mantle wedge beneath eastern China and a new lithospheric thinning mechanism of the North China craton-Geodynamic effects of deep recycled carbon. Sci. China Earth Sci. 61 (7), 853–868.
Li, C., et al., 2012a. 3D geophysical characterization of the Sulu–Dabie orogen and its environs. Phys. Earth Planet. Inter. 192, 35–53.
Li, S., Zhao, G., Dai, L., Zhou, L., Liu, X., Suo, Y., Santosh, M., 2012b. Cenozoic faulting of the Bohai Bay Basin and its bearing on the destruction of the eastern North China Craton. J. Asian Earth Sci. 47, 80–93.
Li, J., Zhang, Y., Dong, S., Johnston, S.T., 2014. Cretaceous tectonic evolution of South China: A preliminary synthesis. Earth Sci. Rev. 134, 98–136.
Li, X., et al., 2015. Has the Yangtze craton lost its root? A comparison between the North China and Yangtze cratons. Tectonophysics 655, 1–14.
Li, S., Suo, Y., Li, X., Zhou, J., Santosh, M., Wang, P., Zhang, G., 2019. Mesozoic tectono-magmatic response in the East Asian ocean-continent connection zone to subduction of the Paleo-Pacific Plate. Earth Sci. Rev. 192, 91–137.
Li, B., et al., 2020. Cenozoic multi-phase deformation in the Qilian Shan and out-of-sequence development of the northern Tibetan Plateau. Tectonophysics 782, 228423.
Lin, W., Wei, W., 2020. Late Mesozoic extensional tectonics in the North China Craton and its adjacent regions: a review and synthesis. Int. Geol. Rev. 62 (7-8), 811–839.
Lin, W., et al., 2013. Late Mesozoic compressional to extensional tectonics in the Yiwulüshan massif, NE China and its bearing on the evolution of the Yinshan–Yanshan orogenic belt: Part I: Structural analyses and geochronological constraints. Gondwana Res. 23 (1), 54–77.
Liu, S., Nummedal, D., 2004. Late Cretaceous subsidence in Wyoming: Quantifying the dynamic component. Geology 32 (5), 397–400.
Liu, J., Han, J., Fyfe, W.S., 2001. Cenozoic episodic volcanism and continental rifting in northeast China and possible link to Japan Sea development as revealed from K–Ar geochronology. Tectonophysics 339 (3-4), 385–401.
Liu, S., Steel, R., Zhang, G., 2005. Mesozoic sedimentary basin development and tectonic implication, northern Yangtze Block, eastern China: record of continent–continent collision. J. Asian Earth Sci. 25 (1), 9–27.
Liu, L., Spasojević, S., Gurnis, M., 2008. Reconstructing Farallon plate subduction beneath North America back to the Late Cretaceous. Science 322 (5903), 934–938.
Liu, L., Gurnis, M., Seton, M., Saleeby, J., Müller, R.D., Jackson, J.M., 2010. The role of oceanic plateau subduction in the Laramide orogeny. Nat. Geosci. 3 (5), 353–357.
Liu, S., Nummedal, D., Liu, L., 2011. Migration of dynamic subsidence across the Late Cretaceous United States Western Interior Basin in response to Farallon plate subduction. Geology 39 (6), 555–558.
Liu, S., Su, S., Zhang, G., 2013. Early Mesozoic basin development in North China: Indications of cratonic deformation. J. Asian Earth Sci. 62, 221–236.
Liu, S., Qian, T., Li, W., Dou, G., Wu, P., 2015. Oblique closure of the northeastern Paleo-Tethys in central China. Tectonics 34 (3), 413–434.
Liu, S., Gurnis, M., Ma, P., Zhang, B., 2017a. Reconstruction of northeast Asian deformation integrated with western Pacific plate subduction since 200 Ma. Earth Sci. Rev. 175, 114–142.
Liu, X., Zhao, D., 2016. P and S wave tomography of Japan subduction zone from joint inversions of local and teleseismic travel times and surface-wave data. Phys. Earth Planet. Inter. 252, 1–22.
Liu, X., Zhao, D., Li, S., Wei, W., 2017b. Age of the subducting Pacific slab beneath East Asia and its geodynamic implications. Earth Planet. Sci. Lett. 464, 166–174.
Liu, S., Lin, C., Liu, X., Zhuang, Q., 2018. Syn-tectonic sedimentation and its linkage to fold-thrusting in the region of Zhangjiakou, North Hebei, China. Sci. China Earth Sci. 61 (6), 681–710.
Liu, J., Cai, R., Pearson, D.G., Scott, J.M., 2019. Thinning and destruction of the lithospheric mantle root beneath the North China Craton: A review. Earth Sci. Rev. 196, 102873.
Liu, Y., Liu, L., Wu, Z., Li, W., Hao, X., 2020. New insight into East Asian tectonism since the late Mesozoic inferred from erratic inversions of NW-trending faulting within the Bohai Bay Basin. Gondwana Res.
Liu, L., Peng, D., Liu, L., Chen, L., Li, S., Wang, Y., Feng, M., 2021a. East Asian lithospheric evolution dictated by multistage Mesozoic flat-slab subduction. Earth Sci. Rev. 103621.
Liu, L., Liu, L., Xu, Y.G., 2021b. Mesozoic intraplate tectonism of East Asia due to flat subduction of a composite Yanshanian slab. Earth Sci. Rev. 103505.
Liu, S., Zhang, A., Lin, C., Zhang, B., Yuan, H., Huang, D., Horton, B.K., 2021c. Thrust duplexing and transpression in the Yanshan Mountains: Implications for early Mesozoic orogenesis and decratonization of the North China Craton. Basin Res. 1–25.
Liu, S., Ma, P., Zhang, B., Gurnis, M., 2021d. The Horizontal Slab Beneath East Asia and Its Subdued Surface Dynamic Response. J. Geophys. Res. Solid Earth 126 (3) e2020JB021156.
Ma, P., Liu, S., Gurnis, M., Zhang, B., 2019. Slab horizontal subduction and slab tearing beneath East Asia. Geophys. Res. Lett. 46 (10), 5161–5169.
Meng, Q., Wu, G., Fan, L., Wei, H., 2019. Tectonic evolution of early Mesozoic sedimentary basins in the North China block. Earth Sci. Rev. 190, 416–438.

Mercier, J.L., Hou, M., Vergély, P., Wang, Y., 2007. Structural and stratigraphical constraints on the kinematics history of the Southern Tan–Lu Fault Zone during the Mesozoic Anhui Province, China. Tectonophysics 439 (1-4), 33–66.
Mercier, J.L., et al., 2013a. Structural records of the late Cretaceous-Cenozoic extension in Eastern China and the kinematics of the Southern Tan-Lu and Qinling fault zone (Anhui and Shaanxi provinces, PR China). Tectonophysics 582, 50–75.
Mercier, J.L., et al., 2013b. Structural records of the late Cretaceous–Cenozoic extension in Eastern China and the kinematics of the Southern Tan-Lu and Qinling fault zone (Anhui and Shaanxi provinces, PR China). Tectonophysics 582, 50–75.
Metcalfe, I., 2006. Palaeozoic and Mesozoic tectonic evolution and palaeogeography of East Asian crustal fragments: the Korean Peninsula in context. Gondwana Res. 9 (1-2), 24–46.
Molnar, P., Atwater, T., 1978. Interarc spreading and Cordilleran tectonics as alternates related to the age of subducted oceanic lithosphere. Earth Planet. Sci. Lett. 41 (3), 330–340.
Molnar, P., England, P., Martinod, J., 1993. Mantle dynamics, uplift of the Tibetan Plateau, and the Indian monsoon. Rev. Geophys. 31 (4), 357–396.
Müller, R.D., et al., 2016. Ocean basin evolution and global-scale plate reorganization events since Pangea breakup. Annu. Rev. Earth Planet. Sci. 44, 107–138.
Müller, R.D., Zahirovic, S., Williams, S.E., Cannon, J., Seton, M., Bower, D.J., Gurnis, M., 2019. A global plate model including lithospheric deformation along major rifts and orogens since the Triassic. Tectonics 38 (6), 1884–1907.
Nakakuki, T., Mura, E., 2013. Dynamics of slab rollback and induced back-arc basin formation. Earth Planet. Sci. Lett. 361, 287–297.
Northrup, C.J., Royden, L.H., Burchfiel, B.C., 1995. Motion of the Pacific plate relative to Eurasia and its potential relation to Cenozoic extension along the eastern margin of Eurasia. Geology 23 (8), 719–722.
O'Connor, J.M., et al., 2013. Constraints on past plate and mantle motion from new ages for the Hawaiian-Emperor Seamount Chain. Geochem. Geophys. Geosyst. 14 (10), 4564–4584.
Ouimet, W., Whipple, K., Royden, L., Reiners, P., Hodges, K., Pringle, M., 2010. Regional incision of the eastern margin of the Tibetan Plateau. Lithosphere 2 (1), 50–63.
Pang, Y., et al., 2018. The Mesozoic-Cenozoic igneous intrusions and related sediment-dominated hydrothermal activities in the South Yellow Sea Basin, the Western Pacific continental margin. J. Mar. Syst. 180, 152–161.
Qi, J., Yang, Q., 2010. Cenozoic structural deformation and dynamic processes of the Bohai Bay basin province, China. Mar. Pet. Geol. 27 (4), 757–771.
Ren, J., Tamaki, K., Li, S., Junxia, Z., 2002. Late Mesozoic and Cenozoic rifting and its dynamic setting in Eastern China and adjacent areas. Tectonophysics 344 (3-4), 175–205.
Ribe, N.M., 2010. Bending mechanics and mode selection in free subduction: A thin-sheet analysis. Geophys. J. Int. 180 (2), 559–576.
Ribe, N.M., Stutzmann, E., Ren, Y., Van Der Hilst, R., 2007. Buckling instabilities of subducted lithosphere beneath the transition zone. Earth Planet. Sci. Lett. 254 (1–2), 173–179.
Richards, M.A., Engebretson, D.C., 1992. Large-scale mantle convection and the history of subduction. Nature 355 (6359), 437–440.
Saleeby, J., 2003. Segmentation of the Laramide slab—Evidence from the southern Sierra Nevada region[J]. Geol. Soc. Am. Bull., 2003 115 (6), 655–668.
Salze, M., Martinod, J., Guillaume, B., Kermarrec, J.J., Ghiglione, M.C., Sue, C., 2018. Trench-parallel spreading ridge subduction and its consequences for the geological evolution of the overriding plate: insights from analogue models and comparison with the Neogene subduction beneath Patagonia. Tectonophysics 737, 27–39.
Sandwell, D., et al., 2013. Toward 1-mGal accuracy in global marine gravity from CryoSat-2, Envisat, and Jason-1. Lead. Edge 32 (8), 892–899.
Schellart, W.P., Lister, G.S., 2005a. The role of the East Asian active margin in widespread extensional and strike-slip deformation in East Asia. J. Geol. Soc. 162 (6), 959–972.
Schellart, W.P., Lister, G.S., 2005b. The role of the East Asian active margin in widespread extensional and strike-slip deformation in East Asia. J. Geol. Soc. 162 (6), 959–972.
SDBGMR Shandong Bureau of Geology and Mineral Resources, 1991. Regional Geology of Shangdong Province. Geological Publishing House, Beijing, pp. 1–594.
Sdrolias, M., Müller, R.D., 2006. Controls on back-arc basin formation. Geochem. Geophys. Geosyst. 7 (4).
Seton, M., et al., 2012. Global continental and ocean basin reconstructions since 200 Ma. Earth Sci. Rev. 113 (3-4), 212–270.
Seton, M., et al., 2015. Ridge subduction sparked reorganization of the Pacific plate-mantle system 60–50 million years ago. Geophys. Res. Lett. 42 (6), 1732–1740.
Shen, C., Hu, D., Shao, C., Mei, L., 2018. Thermochronology quantifying exhumation history of the Wudang Complex in the South Qinling Orogenic Belt, central China. Geol. Mag. 155 (4), 893–906.
Shinn, Y.J., Chough, S.K., Hwang, I.G., 2010. Structural development and tectonic evolution of Gunsan Basin (Cretaceous–Tertiary) in the central Yellow Sea. Mar. Pet. Geol. 27 (2), 500–514.
Shu, L., Charvet, J., 1996. Kinematics and geochronology of the Proterozoic Dongxiang-Shexian ductile shear zone: with HP metamorphism and ophiolitic melange (Jiangnan Region, South China). Tectonophysics 267 (1-4), 291–302.
Shu, L., et al., 1991. Structural analysis of the Nanchang-Wanzai sinistral ductile shear zone (Jiangnan region, South China). J. SE Asian Earth Sci. 6 (1), 13–23.
Shu, L., Faure, M., Wang, B., Zhou, X., Song, B., 2008. Late Palaeozoic–Early Mesozoic geological features of South China: response to the Indosinian collision events in Southeast Asia. Comptes. Rendus. Geosci. 340 (2–3), 151–165.
Sonder, L.J., Jones, C.H., 1999. Western United States extension: How the west was widened. Annu. Rev. Earth Planet. Sci. 27 (1), 417–462.
Styron, R., Taylor, M., Sundell, K., 2015. Accelerated extension of Tibet linked to the northward underthrusting of Indian crust. Nat. Geosci. 8 (2), 131–134.
Su, J., Zhu, W., Chen, J., Ge, R., Zheng, B., Min, B., 2014. Cenozoic inversion of the East China Sea Shelf Basin: implications for reconstructing Cenozoic tectonics of eastern China. Int. Geol. Rev. 56 (12), 1541–1555.
Suo, Y., et al., 2014. Cenozoic tectonic jumping and implications for hydrocarbon accumulation in basins in the East Asia Continental Margin. J. Asian Earth Sci. 88, 28–40.
Suo, Y.H., Li, S.Z., Cao, X., Wang, X., Somerville, L., Wang, G., Wang, P., Liu, B., 2020. Mesozoic-Cenozoic basin inversion and geodynamics in East China: a review. Earth Sci. Rev. 103357.
Tagawa, M., Nakakuki, T., Tajima, F., 2007. Dynamical modeling of trench retreat driven by the slab interaction with the mantle transition zone[J]. Earth, planets and space 59 (2), 65–74.
Tang, J., Xu, W., Wang, F., Ge, W., 2018. Subduction history of the Paleo-Pacific slab beneath Eurasian continent: Mesozoic-Paleogene magmatic records in Northeast Asia. Sci. China Earth Sci. 61 (5), 527–559.
Zhang, T., 2014. Structural deformation characteristics of lower yangtze region and its potential for the preservation of shale gas. [Master Thesis] Nanjing Univeristy, Nanjing, China, 1-85.
Tapponnier, P. et al., 2001. Oblique stepwise rise and growth of the Tibet Plateau. science, 294(5547): 1671-1677.
Tian, Y., Kohn, B.P., Hu, S., Gleadow, A.J., 2015. Synchronous fluvial response to surface uplift in the eastern Tibetan Plateau: Implications for crustal dynamics. Geophys. Res. Lett. 42 (1), 29–35.
Torsvik, T.H., et al., 2017. Pacific plate motion change caused the Hawaiian-Emperor Bend. Nat. Commun. 8 (1), 1–12.
Van Hinsbergen, D.J., et al., 2012. Greater India Basin hypothesis and a two-stage Cenozoic collision between India and Asia. Proc. Natl. Acad. Sci. 109 (20), 7659–7664.
Waldron, J.W., 2005. Extensional fault arrays in strike-slip and transtension. J. Struct. Geol. 27 (1), 23–34.
Wan, T.F., 2013. A new Asian tectonic unit map. Geol. China 40 (5), 1351–1365.
Wang, Y., 2006. The onset of the Tan–Lu fault movement in eastern China: constraints from zircon (SHRIMP) and $^{40}Ar/^{39}Ar$ dating. Terra Nova 18 (6), 423–431.
Wang, P., et al., 2012. Yanshanian fold-thrust tectonics and dynamics in the Middle-Lower Yangtze River area, China. Acta Petrol. Sin. 28 (10), 3418–3430.
Wang, L., Cheng, F., Zuza, A.V., Jolivet, M., Liu, Y., Guo, Z., Li, X., Zhang, C., 2021. Diachronous growth of the northern Tibetan plateau derived from flexural modeling. Geophys. Res. Lett. 48 (8), e2020GL092346.
Wang, F., Xu, Y.G., Xu, W.L., Wu, W., Sun, C.Y., 2017. Early Jurassic calc-alkaline magmatism in northeast China: Magmatic response to subduction of the Paleo-Pacific Plate beneath the Eurasian continent. J. Asian Earth Sci. 143, 249–268.
Wang, W., et al., 2018. Age, provenance and tectonic setting of Neoproterozoic to early Paleozoic sequences in southeastern South China Block: Constraints on its linkage to western Australia-East Antarctica. Precambrian Res. 309, 290–308.
Watson, M.P., Hayward, A.B., Parkinson, D.N., Zhang, Z.M., 1987. Plate tectonic history, basin development and petroleum source rock deposition onshore China. Mar. Pet. Geol. 4 (3), 205–225.
Webb, A.A.G., et al., 2017. The Himalaya in 3D: Slab dynamics controlled mountain building and monsoon intensification. Lithosphere 9 (4), 637–651.
Wei, W., Xu, J., Zhao, D., Shi, Y., 2012. East Asia mantle tomography: New insight into plate subduction and intraplate volcanism. J. Asian Earth Sci. 60, 88–103.
Zhu, W.L., Zhong, K., Fu, X.W., Cheng, C.F., Zheng, M.Q., Gao, S.L., 2019. The formation and evolution of the East China Sea Shelf Basin: A new view. Earth-Sci. Rev. 190, 89–111.
Wessel, P., Smith, W.H., 1998. New, improved version of Generic Mapping Tools released. *Eos*. Transactions American Geophysical Union 79 (47), 579.
Whittaker, J.M., et al., 2007. Major Australian-Antarctic plate reorganization at Hawaiian-Emperor bend time. Science 318 (5847), 83–86.
Wilson, T.J., 1991. Transition from back-arc to foreland basin development in the southernmost Andes: Stratigraphic record from the Ultima Esperanza District, Chile. Geol. Soc. Am. Bull. 103 (1), 98–111.
Wu, G., 2019. The Yanshanian Orogeny and Two Kinds of Yanshanides in Eastern Central China. Acta Geologica Sinica English Edition 79 (4), 507–518.
Wu, J.T., Wu, J., 2019. Izanagi-Pacific ridge subduction revealed by a 56 to 46 Ma magmatic gap along the northeast Asian margin. Geology 47 (10), 953–957.
Wu, J., Suppe, J., Lu, R., Kanda, R., 2016. Philippine Sea and East Asian plate tectonics since 52 Ma constrained by new subducted slab reconstruction methods. J. Geophys. Res. Solid Earth 121 (6), 4670–4741.
Wu, L., et al., 2018a. Deciphering the origin of the Cenozoic intracontinental rifting and volcanism in eastern China using integrated evidence from the Jianghan Basin. Gondwana Res. 64, 67–83.
Wu, L., et al., 2018b. The stratigraphic and structural record of the Cretaceous Jianghan Basin, central China: Implications for initial rifting processes and geodynamics. Cretac. Res. 90, 21–39.
Wu, F., Yang, J., Xu, Y., Wilde, S.A., Walker, R.J., 2019. Destruction of the North China craton in the Mesozoic. Annu. Rev. Earth Planet. Sci. 47, 173–195.
Xie, F.R., Cui, X.F., Zhao, J.T., Chen, Q.C., Li, H., 2004. Regional division of the recent tectonic stress field in China and adjacent areas. Chin. J. Geophys. 47, 654–662.
Xiong, S., Tong, J., Ding, Y., Li, Z., 2016. Aeromagnetic data and geological structure of continental China: A review. Appl. Geophys. 13 (2), 227–237.
Xu, Z., 2003. Exhumation structure and mechanism of the Sulu ultrahigh-pressure metamorphic belt, central China. Acta Geol. Sin. 77, 432–450.
Xu, Y., 2007. Diachronous lithospheric thinning of the North China Craton and formation of the Daxin'anling–Taihangshan gravity lineament. Lithos 96 (1-2), 281–298.

Xu, X., Gao, S., 2015a. The structure and formation of the Cenozoic fault basin in the Lower Yangtze region. Earth Sci. Front. 22 (6), 148–166.
Xu, J., Zhu, G., 1994. Tectonic models of the Tan-Lu fault zone, eastern China. Int. Geol. Rev. 36 (8), 771–784.
Xu, J., Zhu, G., Tong, W., Cui, K., Liu, Q., 1987. Formation and evolution of the Tancheng-Lujiang wrench fault system: a major shear system to the northwest of the Pacific Ocean. Tectonophysics 134 (4), 273–310.
Xu, Y., Li, Z.W., Liu, J.S., Hao, T.Y., 2008a. Pn wave velocity and anisotropy in the Yellow Sea and adjacent region. Chin. J. Geophys. 51 (5), 1015–1022.
Xu, Q., Ji, J., Wang, J., Wang, Z., Han, W., Yu, J., 2008b. Active mode of the Tan-Lu fault zone in Early Cenozoic. Chin. J. Geol. 43 (2), 402–414.
Xu, J.R., Zhao, Z.X., Ishikawa, Y.Z., 2008c. Regional characteristics of crustal stress field and tectonic motions in and around Chinese mainland. Chin. J. Geophys. 51, 770–781.
Xu, X., Gao, S.L., Wang, X.J., 2015b. Cenozoic Deformation of Extensional Tectonics in the Lower Yangtze Region and Its Tectonic Significance. Earth Sci.—J. China Univ. Geosci. 40 (12), 1968–1986.
Xu, X., et al., 2018. Structure and sedimentary characteristics of the Meso-Cenozoic basin group along the Yangtze River in the Lower Yangtze region. Pet. Geol. Exp. 03 (2018), 303–314.
Yang, Y., 2013. An unrecognized major collision of the Okhotomorsk Block with East Asia during the Late Cretaceous, constraints on the plate reorganization of the Northwest Pacific. Earth Sci. Rev. 126, 96–115.
Yang, J., et al., 2005. Two ultrahigh-pressure metamorphic events recognized in the central orogenic belt of China: Evidence from the U-Pb dating of coesite-bearing zircons. Int. Geol. Rev. 47 (4), 327–343.
Yang, T., Gurnis, M., Zahirovic, S., 2018a. Slab avalanche-induced tectonics in self-consistent dynamic models. Tectonophysics 746, 251–265.
Yang, T., Moresi, L., Zhao, D., Sandiford, D., Whittaker, J., 2018b. Cenozoic lithospheric deformation in Northeast Asia and the rapidly-aging Pacific Plate. Earth Planet. Sci. Lett. 492, 1–11.
Yang, T., Liu, S., Guo, P., Leng, W., Yang, A., 2020. Yanshanian orogeny during North China's drifting away from the trench: Implications of numerical models. Tectonics 39 (12) e2020TC006350.
Yao, Y., et al., 2010. Tectonic evolution and hydrocarbon potential in northern area of the South Yellow Sea. J. Earth Sci. 21 (1), 71–82.
Yin, A., 2010. Cenozoic tectonic evolution of Asia: A preliminary synthesis. Tectonophysics 488 (1-4), 293–325.
Yin, A., Harrison, T.M., 2000. Geologic evolution of the Himalayan-Tibetan orogen. Annu. Rev. Earth Planet. Sci. 28 (1), 211–280.
Yin, A., et al., 1999. Tertiary deformation history of southeastern and southwestern Tibet during the Indo-Asian collision. Geol. Soc. Am. Bull. 111 (11), 1644–1664.
Yin, A., et al., 2008. Cenozoic tectonic evolution of Qaidam basin and its surrounding regions (Part 1): The southern Qilian Shan-Nan Shan thrust belt and northern Qaidam basin. Geol. Soc. Am. Bull. 120 (7-8), 813–846.
Yin, A., Nie, S., 1993. An indentation model for the North and South China collision and the development of the Tan-Lu and Honam fault systems, eastern Asia. Tectonics 12 (4), 801–813.
Yoon, Y., et al., 2010. Cross-section restoration and one-dimensional basin modeling of the Central Subbasin in the southern Kunsan Basin, Yellow Sea. Mar. Pet. Geol. 27 (7), 1325–1339.
Zahirovic, S., Seton, M., Müller, R.D., 2014. The cretaceous and cenozoic tectonic evolution of Southeast Asia. Solid Earth 5 (1), 227–273.
Zhang, K., 1997. North and South China collision along the eastern and southern North China margins. Tectonophysics 270 (1-2), 145–156.
Zhang, Y., Ma, Y., Yang, N., Shi, W., Dong, S., 2003. Cenozoic extensional stress evolution in North China. J. Geodyn. 36 (5), 591–613.
Zhang, G., Dong, Y., Lai, S., Guo, A., Meng, Q., Liu, S., Li, S., 2004. Mianlue tectonic zone and Mianlue suture zone on southern margin of Qinling-Dabie orogenic belt. Sci. China Series D- Earth Sci. 47 (4), 300–316.
Zhang, M., Xu, D., Chen, J., 2007. Geological structure of the Yellow Sea Area from regional gravity and magnetic interpretation. Appl. Geophys. 4 (2), 75–83.
Zhang, T., et al., 2013. Structural deformation characteristics and shale gas preservation of lower Yangtze region. J. China Coal Soc. 38 (5), 883–889.
Zhang, F., Dilek, Y., Chen, H., Yang, S., Meng, Q., 2017. Structural architecture and stratigraphic record of Late Mesozoic sedimentary basins in NE China: Tectonic archives of the Late Cretaceous continental margin evolution in East Asia. Earth Sci. Rev. 171, 598–620.
Zhao, X., Coe, R.S., 1987. Palaeomagnetic constraints on the collision and rotation of North and South China. Nature 327 (6118), 141–144.
Zhao, D., Ohtani, E., 2009. Deep slab subduction and dehydration and their geodynamic consequences: evidence from seismology and mineral physics. Gondwana Res. 16 (3-4), 401–413.
Zhao, D., Yanada, T., Hasegawa, A., Umino, N., Wei, W., 2012. Imaging the subducting slabs and mantle upwelling under the Japan Islands. Geophys. J. Int. 190 (2), 816–828.
Zhao, T., Zhu, G., Lin, S., Wang, H., 2016. Indentation-induced tearing of a subducting continent: evidence from the Tan–Lu fault zone, East China. Earth Sci. Rev. 152, 14–36.
Zheng, J., Dai, H., 2018. Subduction and retreating of the western Pacific plate resulted in lithospheric mantle replacement and coupled basin-mountain respond in the North China Craton. Sci. China Earth Sci. 61 (4), 406–424.
Zheng, Y., Fu, B., Gong, B., Li, L., 2003. Stable isotope geochemistry of ultrahigh pressure metamorphic rocks from the Dabie–Sulu orogen in China: implications for geodynamics and fluid regime. Earth Sci. Rev. 62 (1-2), 105–161.
Zheng, Y., Zhou, J., Wu, Y., Xie, Z., 2005. Low-grade metamorphic rocks in the Dabie-Sulu orogenic belt: A passive-margin accretionary wedge deformed during continent subduction. Int. Geol. Rev. 47 (8), 851–871.
Zheng, T.Y., Zhao, L., Xu, W.W., Zhu, R.X., 2008. Insight into modification of North China Craton from seismological study in the Shandong Province. Geophys. Res. Lett. 35 (22).
Zheng, H., et al., 2013. Pre-miocene birth of the Yangtze River. Proc. Natl. Acad. Sci. 110 (19), 7556–7561.
Zhu, G., Xu, J., Liu, G., 1999. Tectonic Pattern and Dynamic Mechanism of Foreland Deformation in the Lower Yangtze Region. Gondwana Res. 4 (2), 557–559.
Zhu, G., Liu, G., Dunlap, W.J., Teyssier, C., Wang, Y., Niu, M., 2004. $^{40}Ar/^{39}Ar$ geochronological constraints on syn-orogenic strike-slip movement of Tan-Lu fault zone. Chin. Sci. Bull. 49 (5), 499–508.
Zhu, G., Wang, Y., Liu, G., Niu, M., Xie, C., Li, C., 2005. $^{40}Ar/^{39}Ar$ dating of strike-slip motion on the Tan–Lu fault zone, East China. J. Struct. Geol. 27 (8), 1379–1398.
Zhu, G., Liu, G.S., Niu, M.L., Xie, C.L., Wang, Y.S., Xiang, B., 2009a. Syn-collisional transform faulting of the Tan-Lu fault zone, East China. Int. J. Earth Sci. 98 (1), 135–155.
Zhu, W.L., Mi, L.J., Gong, Z.S., et al., 2009b. Hydrocarbon Accumulation and Exploration Offshore the Bohai Sea. Science Press, Beijing, pp. 1–368.
Zhu, W.L., Mi, L.J., et al., 2010. Atlas of Oil and Gas Basins, China Sea. Petroleum Industry Press, Beijing, pp. 1–316.
Zhong, S., Gurnis, M., 1995. Mantle convection with plates and mobile, faulted plate margins. Science 267 (5199), 838–843.
Zhu, G., Jiang, D., Zhang, B., Chen, Y., 2012. Destruction of the eastern North China Craton in a backarc setting: Evidence from crustal deformation kinematics. Gondwana Res. 22 (1), 86–103.
Zhu, G., Liu, C., Gu, C., Zhang, S., Li, Y., Su, N., Xiao, S., 2018. Oceanic plate subduction history in the western Pacific Ocean: Constraint from late Mesozoic evolution of the Tan-Lu Fault Zone. Sci. China Earth Sci. 61 (4), 386–405.
Zhu, Y., Liu, S., Zhang, B., Gurnis, M., Ma, P., 2021. Reconstruction of the cenozoic deformation of the Bohai Bay Basin, north China. Basin Res. 33 (1), 364–381.
Ziegler, P.A., Cloetingh, S., 2004. Dynamic processes controlling evolution of rifted basins. Earth Sci. Rev. 64 (1-2), 1–50.
ZJBGMR Zhejiang Bureau of Geology and Mineral Resources, 1989. Regional Geology of Zhejiang Province. Geological Publishing House, Beijing, pp. 1–688.
Zuza, A.V., Yin, A., 2016. Continental deformation accommodated by non-rigid passive bookshelf faulting: An example from the Cenozoic tectonic development of northern Tibet. Tectonophysics 677, 227–240.